

On Hamiltonian Dynamics of a Chain of Rigid Bodies

A thesis submitted
in partial fulfillment of the requirements
for the degree of
Bachelor-Master of Technology (Dual Degree)

by

VIKASH CHAURASIA



to the
DEPARTMENT OF MECHANICAL ENGINEERING
INDIAN INSTITUTE OF TECHNOLOGY KANPUR

May 2012

Certificate

It is certified that the work contained in this thesis entitled “*On Hamiltonian Dynamics of a chain of Rigid bodies* ” has been carried out by *Vikash Chaurasia (Roll No. Y7027500)* under my supervision and that this work has not been submitted elsewhere for a degree.

Dr. Basant Lal Sharma
Assistant Professor
Department of Mechanical Engineering
Indian Institute of Technology Kanpur

May 2012

“Hard work and Sincerity will fetch you anything, just anything”

My Dad

Abstract

This thesis contains the Hamiltonian formulation of a chain of identical rigid bodies with nearest neighbour interaction and presents numerical results for the corresponding dynamics based on a symplectic algorithm. The (finite) rotation of rigid bodies has been described using the matrix representation as well as unit quaternion based representation of the special rotation group. In both representations, the accompanying rigid body constraints, which are holonomic, have been incorporated through Lagrange multipliers. For example this has been done to capture the unit quaternion constraint. The (constrained) Hamiltons equations have been solved using some existing symplectic algorithms. The numerical algorithms for the constrained problem conserve its symplectic structure.

Acknowledgements

I would like to express my sincere gratitude to my supervisor, Dr. Basant Lal sharma for his ideas, guidance and suggestions. Without his valuable guidance, this work would never have been successful. His pristine approach toward research inspire me to work honestly, ethically and think independently. I am thankful for his patience and trust in me, when I was slow and low.

I would like to thank Dr. Ishan Sharma for showing me the glimpse of mechanics and mathematics and encouraging me to do research. I am thankful to my seniors Suhail and Anup da for their guidance. Discussion with them has been very helpful in my research work.

I would like to thank my friends and colleagues for their constant help and encouragement. I would like to thank my awesome wingies Arpan, Alok, Hitanshu, Pulkit, Boxer, Lohan, Baba, Jais, Gauss, Ayush, Kamla, Deepesh, Siddharth, Tekari, Nikhil, Ambu, Sandy and Ashu for making my stay at college memorable. I am especially thankful to my nerdy physics friends Vivek lohani and Siddharth Chandra for whom Physics and Linux are mere grammar. Delightful discussion with them has changed my view on physics and mathematics. I would also like to thank my labmates Navin, Pankaj, Santosh, Surbhit, Mr. Roy, Tanmay da, Paritosh da, Prempal, Uday and Devkant for making the working environment pleasant. Pankaj and Navin are indeed my friends with benefits.

I cannot thank enough my family who love me and trust me more than anybody else in this world. They have always backed me that I can do good things.

Vikash Chaurasia May 2012

Contents

Certificate	i
Abstract	iii
Acknowledgements	iv
List of Figures	vii
1 Introduction	1
1.1 Introduction of rigid body dynamics	1
1.2 Literature survey	2
2 Numerical experiment	4
2.1 Simple harmonic motion	4
2.2 Non-linear pendulum	6
2.3 Kepler's problem	7
2.4 Galactic orbit	8
2.5 Symmetric top	10
3 Dynamics of three dimensional chain	16
3.1 Rigid body	17
3.2 Hamiltonian formulation using rotation matrix	18
3.2.1 Constraints	20
3.2.2 Hamilton's equations	21
3.2.3 Gradient of Potential	22
3.2.4 Boundary condition	23
3.3 Hamiltonian formulation using quaternion	25
3.3.1 Rotational mass matrix	26
3.3.2 Rotational kinetic energy	28
3.3.3 Potential energy	29
3.3.4 Constraints	29
3.3.5 Hamiltonian	30
3.3.6 Gradient of potential	31
3.3.7 Boundary condition	32
3.3.8 Expression for Lagrange multiplier λ_j	34
3.3.9 Non-Dimensionalisation	35

3.4	Order and Symplecticity of constrained algorithm	36
3.4.1	Order of the constrained algorithm	37
3.4.2	Symplecticity of the constrained algorithm	39
3.5	Example	41
3.5.1	Potential energy	42
4	Conclusion and Future work	46
4.1	Conclusion	46
4.2	Future Work	46
A	Rotation matrix	48
A.1	Rotation matrix in terms of quaternions	48
A.2	Euler angle and quaternions	50
B	RATTLE algorithm	52
C	Proof of Lemma 1	56
	Bibliography	59

List of Figures

1.1	Constraining rigid bodies in a chain [1]	1
1.2	Schematic diagram of a simple graphitic molecular bearing [2]	2
2.1	Hamiltonian (in J) vs time(in sec.)	5
2.2	p vs q, RadauIIA	6
2.3	p vs q, Implicit midpoint	6
2.4	Hamiltonian(in J) vs time(in sec.), RadauIIA	7
2.5	Hamiltonian(in J) vs time(in sec.), Implicit midpoint	7
2.6	Explicit euler	8
2.7	Symplectic Euler	8
2.8	Stormer-verlet	8
2.9	Gauss6	8
2.10	Poincare section, Calculated (left) and Hairer[3] (right)	9
2.11	Hamiltonian(in J) vs time(in sec.) comparison for RK4 and Gauss6	10
2.12	Symmetric body and its axes	11
2.13	3D coordinate of centre of mass	14
2.14	X-Y coordinate of centre of mass	14
2.15	Coordinates of center of mass of top vs time(in sec.)	14
2.16	Angular momentum (in kgm^2s^{-1}) vs time(in sec.)	15
2.17	Hamiltonian of the top(in J) vs time (in sec.)	15
2.18	z coordinate of com	15
2.19	Error in Hamiltonian	15
3.1	three dimensional chain of rigid bodies	16
3.2	Configuration of particles in a rigid body	17
3.3	Error in unit quaternion vs step size for symplectic algorithms	39
3.4	Rigid tetrahedron	42
3.5	Energy(in J) vs number of steps for c1-c2 boundary condition	43
3.6	Energy(in J) vs number of steps for c1-c1 boundary condition	43
3.7	Number of particle n_p vs time for Number of body N =6	44
3.8	Number of body N vs time for number of particle=12	44
3.9	Error in unit quaternion for different bodies	45

Chapter 1

Introduction

1.1 Introduction of rigid body dynamics

Rigid body dynamics find application in wide variety of fields, e.g., robotics, Biomechanics, Granular mechanics, Gaming Industries, Aerospace engineering etc. In almost all the applications, system is considered to be made up of finite number of rigid bodies attached to each other through some interaction.

In robotics, a skeleton is modeled as multi-rigid-bodies system in which rigid bodies are linked to each other through hinge or ball and socket type links. Six-degree freedom manipulators [4] are used to solve the system.

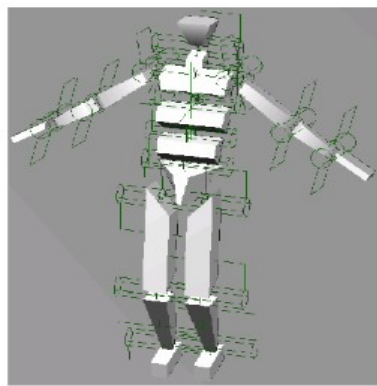


FIGURE 1.1: Constraining rigid bodies in a chain [1]

Using rigid body dynamics algorithms, robot actuator models provide handy tool for handling and analyzing simulation data.

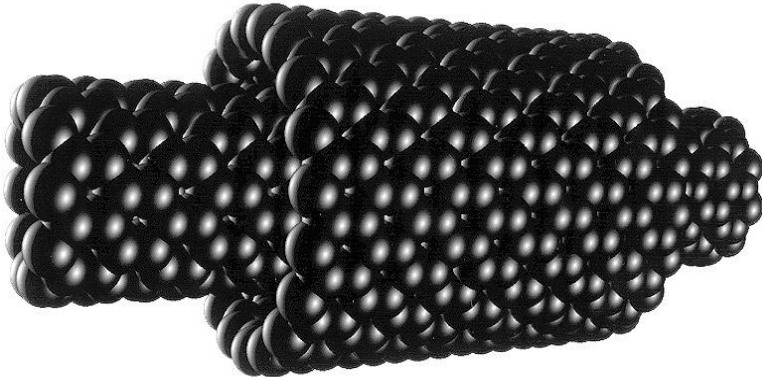


FIGURE 1.2: Schematic diagram of a simple graphitic molecular bearing [2]

One of the recent use of rigid body dynamics includes its application in studying dynamical properties of nanosystems. Simulation of molecular bearings, joints, gears have been done using rigid body dynamics algorithms. These algorithms are found to be very efficient [2], making longer time simulation possible. Figure 1.2 shows graphitic molecular bearing being modeled as pair of nested carbon nanotubes.

In Biomechanics, human body structures are studied by modeling them as chain of rigid bodies, e.g., treatments of inter vertebral disk-degeneration [5] is based on rigid body dynamics. Several rigid body based modeling has been done for chemical compounds, biomolecules such as DNA etc.

With the advent of fast computers, many visualization softwares, based on rigid body dynamics have come up, offering powerful tool for the analysis. Most of the gaming softwares are based on rigid body dynamics using quaternion as rotation parameters. Fast algorithms used in these softwares provide excellent virtual reality platform.

1.2 Literature survey

In rigid body dynamics, several ways of rotation parameterization[6] are used. We get different representation of the equation of motion depending on which parameterization is used. Use of *Euler's angles* to represent rotation comes with the disadvantage of singularity involved in the representation and hence is not the popular choice to study the dynamics of rigid bodies. In this thesis, we use *Rotation matrix* scheme ([7],[8]) and *Quaternion* as rotation parameters. *Quaternion* were proposed long back due to Hamilton [9], but use

of quaternions for studying dynamics of the rigid body was proposed due to Goldstein et al.,[10]. Advantage of using quaternion over traditional methods mainly Euler's angle is that it is singularity free. Also, in contrast to Euler's angle parameterization, which involve trigonometric entities, equation of motion in terms of quaternion turn out to be consisting of algebraic entities which are easier to be solved numerically. One of the disadvantage of using Quaternion is that its length must be kept unity.

Algorithms have been proposed to solve constrained Hamiltonian system (due to unit quaternion constraint), but upto 1st order only. Higher order numerical schemes respecting the unit quaternion constraint are yet to be derived. Several authors ([11],[12],[13]) have studied equation of motion for a single rigid body in terms of *Quaternion*, but the dynamics of chain of rigid bodies of arbitrary shape has not been discussed.

We address the motion of rigid bodies in chain in Hamiltonian formalism in detail. One of the particular focus in this thesis is the use of *augmented* angular velocity and *augmented* inertia matrix in the derivation of invertible *Rotational mass matrix*. Use of augmented matrices is common practice in mechanics based on *Quaternion* algebra. However, derivation of the particular choice of these augmented matrices is absent in the literature. We explain the importance of having invertible rotational mass matrix and show that it is unique.

When Hamilton's equations of dynamical systems are solved numerically using standard ODE solvers, e.g., **ode45**, **Matlab**(adaptive runge kutta method), Hamiltonian of the system blows up in the long time run. This motivate us to use *Symplectic* schemes([14],[15],[16]) for solving Hamilton's equations numerically. In order to force the unit quaternion constraints, standard projection techniques and null-space methods are discussed in the literature. However, using such techniques may destroy the symplectic structure of the system and hence should be used cautiously. Symplectic algorithms for solving multibody system has been addressed([17],[18],[19],[20]). However, the order of discretization discussed is upto 2nd order only.

Chapter 2

Numerical experiment

In this chapter, we give emphasis on importance of using symplectic algorithms([15],[21],[22],[16]). Instead of going into derivation of equations, we discuss the advantage of symplectic algorithms over non-symplectic schemes by means of plots. Each of the example discussed show different advantages of symplectic algorithms.

2.1 Simple harmonic motion

Hamiltonian for this system is given by,

$$H = \frac{p^2}{2m} + \frac{kq^2}{2}.$$

This system is solved for $k = 4N/m$, $m = 1\text{meter}$, initial conditions, $q(0) = 0$ and $p(0) = 2$, step size $h = .01$ and tolerance 10^{-10} . Exact solution of system is,

$$q = \sin(2t), \quad p = 2 \cos(2t).$$

We solve the system using both non-symplectic and symplectic schemes and compare the Hamiltonian for them with the exact solution. The step size and tolerance remain same for all the discussed algorithms.

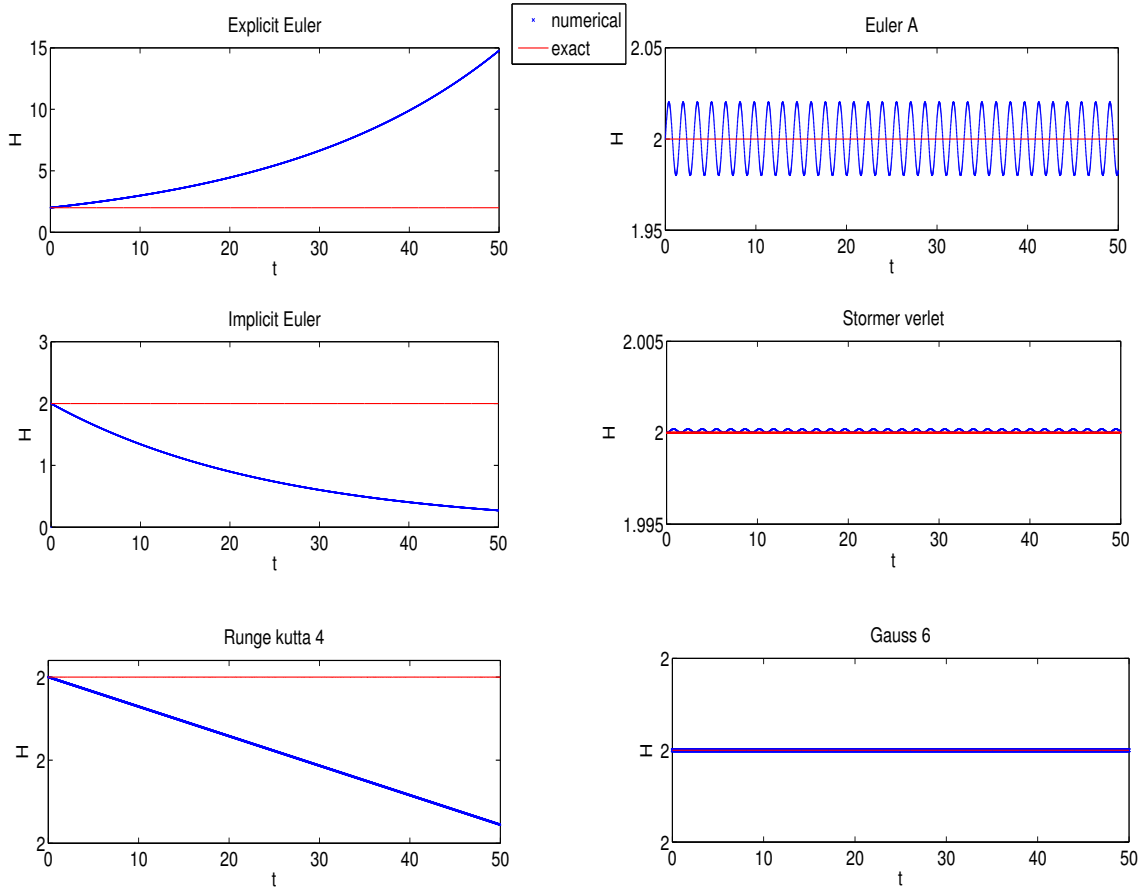


FIGURE 2.1: Hamiltonian (in J) vs time(in sec.)

In the Figure (2.1), plots on left hand side are solutions of non-symplectic schemes, while that on the right side are solutions of symplectic schemes.

Explicit-Euler and *Euler-A* are both the first order algorithms, but in the first case Hamiltonian blows up while in the later case, it remain bounded. For the non-symplectic *Implicit Euler*, Hamiltonian dies out and it again remain bounded in second order symplectic *Stormer-Verlet* scheme. We also observe that the amplitude of oscillation of Hamiltonian is smaller than that in *Euler-A*.

Fourth order *Runge-kutta* seems to conserve the Hamiltonian to a good extent, but Hamiltonian is still declining in comparison to sixth order symplectic *Gauss6* scheme. Significant variation in Hamiltonian can be observed while using *Runge-kutta* scheme, when simulation is done for long time (section 2.4).

We conclude from above discussion that, for same step size and tolerance, symplectic schemes are a better numerical approach than non-symplectic schemes. Also, as the order of symplectic scheme increases, amplitude of variation in Hamiltonian decreases.

2.2 Non-linear pendulum

In order to emphasize on phase space conserving properties of symplectic algorithms, we reproduce here the phase plots for non-linear pendulum, discussed in Hairer, pg314 [3]. Hamiltonian of the system is

$$H = \frac{p^2}{2} - \cos(q) \left(1 - \frac{p}{6}\right).$$

We compare two schemes,

- (a) *Implicit Radau*, non-symplectic scheme of order 3,
- (b) *Implicit Midpoint*, symplectic scheme of order 2,

for initial conditions $p_0 = 0$, $q_0 = -\cos^{-1}(-.8)$ and step size $h = .3$.

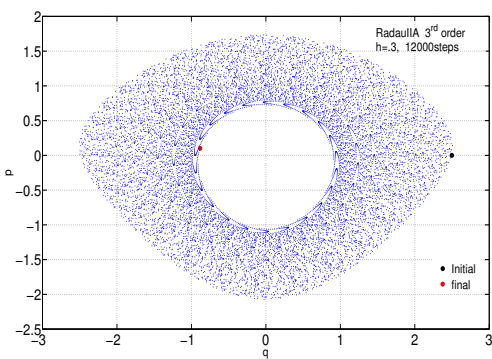


FIGURE 2.2: p vs q , RadauIIA

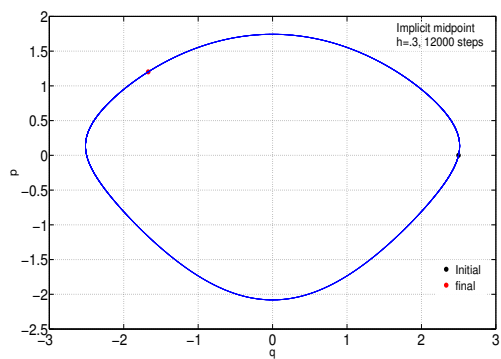


FIGURE 2.3: p vs q , Implicit midpoint

We see from the above phase plots that symplectic methods conserve phase space, while non-symplectic do not. Also, the solution for non-symplectic implicit scheme is dying to zero and would blow up for any non-symplectic explicit scheme.

Energy conserving property of symplectic is clearly seen in plot (2.5). While the Hamiltonian remains bounded in *Implicit-Midpoint* scheme, it keeps decreasing in *Radau* method.

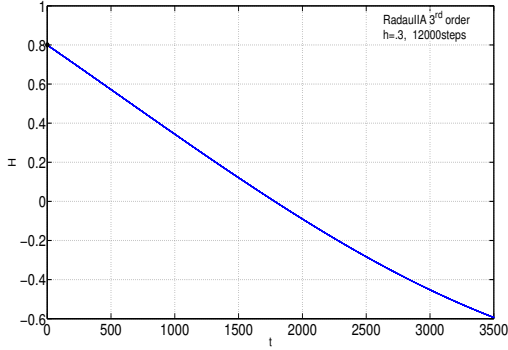


FIGURE 2.4: Hamiltonian(in J) vs time(in sec.), RadauIIA

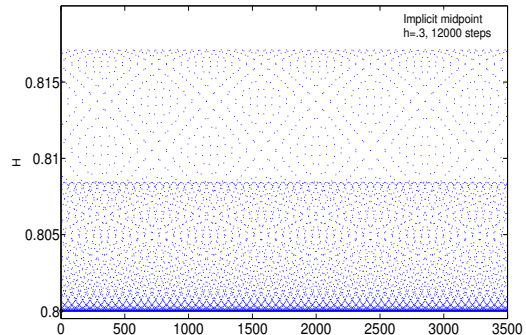


FIGURE 2.5: Hamiltonian(in J) vs time(in sec.), Implicit midpoint

2.3 Kepler's problem

We now analyze here Kepler's problem as another example of highlighting advantage of symplectic schemes over non-symplectic methods. For computing motion of two bodies, which attract each other, one body is assumed to be center. Coordinates of other body is given by $q = (q_1, q_2)$. Hamiltonian for this system is,

$$H = \frac{1}{2}(p_1^2 + p_2^2) - \frac{1}{\sqrt{q_1^2 + q_2^2}}.$$

This system has been solved for initial conditions

$$e = .6, p_1(0) = 0, p_2(0) = \sqrt{\frac{1+e}{1-e}}, q_1(0) = 1 - e, q_2(0) = 0,$$

and compared with exact solution

$$\begin{aligned} q_1(t) &= \frac{(1 - e^2) \cos t}{1 + e \cos(t - t^*)}, \\ q_2(t) &= \frac{(1 - e^2) \sin t}{1 + e \cos(t - t^*)}, \quad t^* = 0. \end{aligned}$$

q_1 vs q_2 (Numerical and exact solution)

We see from figure 2.6 and figure 2.7 that, even for step size 100 times higher than *Explicit Euler*, symplectic *Euler-A* scheme provides more accurate solution. The only disadvantage of *Euler-A* is that, it is a implicit scheme which involves solving nonlinear equations. However,

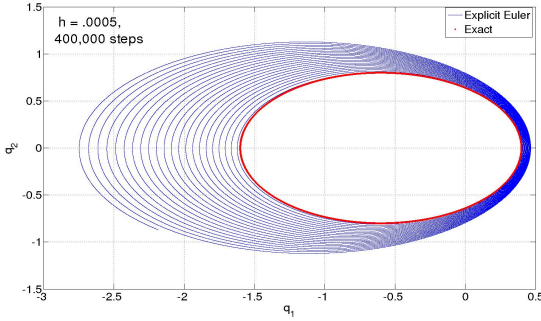


FIGURE 2.6: Explicit euler

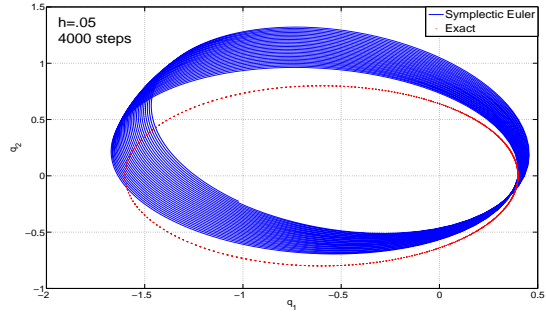


FIGURE 2.7: Symplectic Euler

we find the computation time¹ for *Explicit Euler* to be 51.01 sec., while that for *Euler-A* is 13.71 sec. This demonstrate that symplectic schemes save computation time.

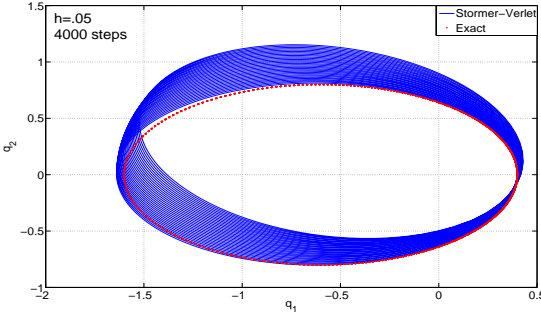


FIGURE 2.8: Stormer-verlet

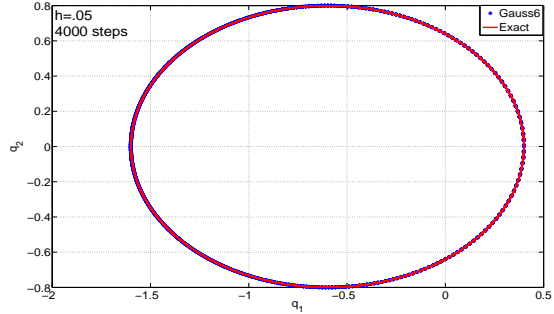


FIGURE 2.9: Gauss6

As we increase the order of symplectic scheme, we get more and more accurate solution. Computation time for *Stormer-Verlet* scheme (figure 2.8) scheme and *Gauss6* schemes (figure 2.9) are 7.26 sec. and 34.09 sec respectively. So, we see from figure 2.6 and figure 2.9 that, sixth order symplectic *Gauss6* scheme give much more accurate solution than *Explicit-Euler* method in lesser computational time.

2.4 Galactic orbit

We discuss here the example of Galactic orbit to demonstrate the Hamiltonian conserving properties of symplectic schemes in long run simulations. We also compare our results with solution given in Hairer, pg322[3].

¹Computation done on a 8 core machine with ‘Intel(R) Xenon cpu ES420 @2.5GHz processor

Hamiltonian for this system is given by

$$H = \frac{1}{2}(p_1^2 + p_2^2 + p_3^2) + \Omega(p_1 q_2 - p_2 q_1) + A \log \left(C + \frac{q_1^2}{a^2} + \frac{q_2^2}{b^2} + \frac{q_3^2}{c^2} \right),$$

where, $(p_i, q_i)_{i=1,2,3}$ are conjugate pairs. Parameters and initial values are

$$a = 1.25, b = 1, c = .5, A = 1, C = 1, \Omega = 0.25,$$

$$q_1(0) = 2.5, q_2(0) = 0, q_3(0) = 0, p_1(0) = 0, p_2(0) = 1.688, p_3(0) = .2$$

Hairer [3] , has discussed Poincare section with the half-plane $q_2 = 0, q_1 > 0, \dot{q}_2 > 0$, for $0 \leq t \leq 10^6$. Number of points captured by such section has been compared with results given in [3].

item	method	order	h	points (Hairer)	points (Calculated)
a)	Gauss	6	1/5	47093	47082
b)	Gauss	6	2/5	46852	46897
c)	Radau	5	1/10	46597	46594
d)	Sungeng	5	1/5	47092	47085
e)	RK4	4	1/40	47004	47003
f)	RK4	4	1/10	46192	46190

TABLE 2.1: No. of points captured in Poincare section

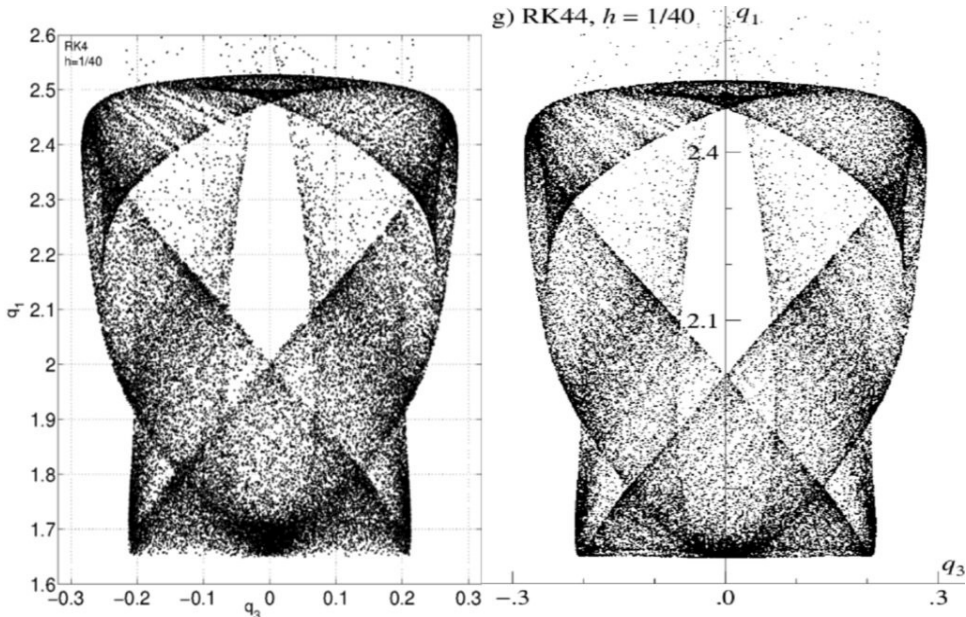


FIGURE 2.10: Poincare section, Calculated (left) and Hairer[3] (right)

Table 2.1 and figure 2.10 show good agreement of our work with published results and hence show our correct implementation of the algorithms. Figure 2.11 clearly shows the advantage

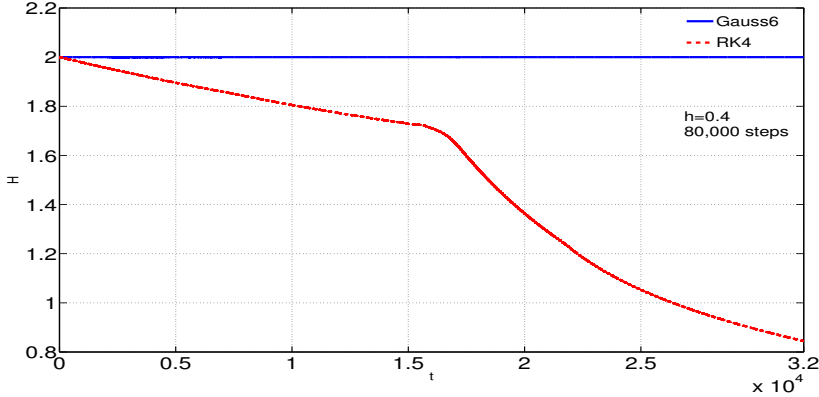


FIGURE 2.11: Hamiltonian(in J) vs time(in sec.) comparison for RK4 and Gauss6

of symplectic *Gauss6* over non-symplectic *RK4* in terms of conserving Hamiltonian. Generally difference between *Gauss6* and *RK4* is not significant in small run or for very small step size, but this simulation for step size $h = 0.4$ and 80,000 steps distinguishes between two schemes. Difference is more and more pronounced as we increases the step size and/or number of steps.

2.5 Symmetric top

In this section, we derive in detail, motion of symmetric body using concept of Euler's angle. In the later part of this section, we demonstrate the symmetric body problem using quaternion and rotation matrix scheme of rotation representation. Figure 2.12 represents schematic of a symmetric body and its orientation in terms of Euler's angle. **XYZ** is the inertial frame and **xyz** is the body fixed frame. **ZYZ** scheme is followed and corresponding rotation matrices (frame rotation) are :

$$\mathbf{R}_z(\psi) = \begin{bmatrix} \cos \psi & \sin \psi & 0 \\ -\sin \psi & \cos \psi & 0 \\ 0 & 0 & 1 \end{bmatrix}, \quad \mathbf{R}_y(\theta) = \begin{bmatrix} \cos \theta & 0 & -\sin \theta \\ 0 & 1 & 0 \\ \sin \theta & 0 & \cos \theta \end{bmatrix}, \quad \mathbf{R}_z(\phi) = \begin{bmatrix} \cos \phi & \sin \phi & 0 \\ -\sin \phi & \cos \phi & 0 \\ 0 & 0 & 1 \end{bmatrix}$$

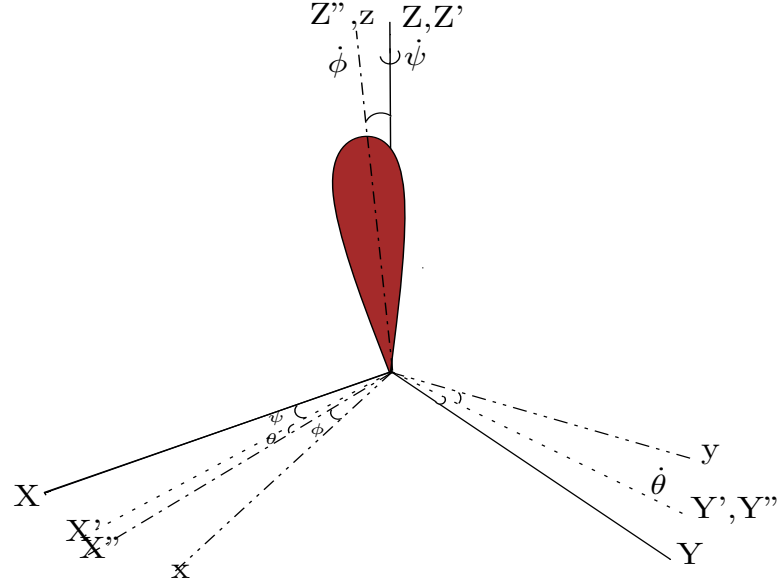


FIGURE 2.12: Symmetric body and its axes

So, rotation matrix for the conversion of a vector from **XYZ** frame to body fixed frame **xyz** is

$$\mathbf{R} = \mathbf{R}_z(\phi)\mathbf{R}_y(\theta)\mathbf{R}_z(\psi) = \begin{bmatrix} \cos \theta \cos \phi \cos \psi - \sin \phi \sin \psi & \cos \theta \cos \phi \sin \psi + \sin \phi \cos \psi & -\cos \phi \sin \theta \\ -\cos \theta \cos \phi \sin \psi - \cos \phi \sin \psi & -\cos \theta \sin \phi \sin \psi + \cos \phi \cos \psi & \sin \phi \sin \theta \\ \sin \theta \cos \psi & \sin \theta \sin \psi & \cos \theta \end{bmatrix}$$

Angular velocity in body fixed frame **xyz** is given by,

$$\omega = \mathbf{R} \begin{bmatrix} 0 \\ 0 \\ \dot{\psi} \end{bmatrix} + \mathbf{R}_z(\phi) \begin{bmatrix} 0 \\ \dot{\theta} \\ 0 \end{bmatrix} + \begin{bmatrix} 0 \\ 0 \\ \dot{\phi} \end{bmatrix}$$

$$\omega = \begin{bmatrix} \dot{\theta} \cos \phi - \dot{\psi} \sin \theta \cos \phi \\ \dot{\theta} \cos \phi + \dot{\psi} \sin \theta \sin \phi \\ \dot{\phi} + \dot{\psi} \cos \theta \end{bmatrix} \quad (2.1)$$

For using Euler's equation, we need to find torque acting on body in body fixed frame.

$$\mathbf{F} = \mathbf{R} \begin{bmatrix} 0 \\ 0 \\ -mg \end{bmatrix} = \begin{bmatrix} mg \cos \phi \sin \theta \\ -mg \sin \phi \sin \theta \\ -mg \cos \theta \end{bmatrix}$$

So, the torque in body fixed frame is $\mathbf{T} = \mathbf{r}_{cm} \times \mathbf{F}$.

$$\mathbf{r}_{cm} = (0, 0, l)^T$$

Therefore, torque is

$$\mathbf{T} = \begin{bmatrix} mgl \sin \phi \sin \theta \\ mgl \cos \phi \sin \theta \\ 0 \end{bmatrix}$$

Let I_1 , I_2 and I_3 be moment of inertia along principle axis of the top. Using Euler's equation for motion,

$$I_1 \frac{d\omega_x}{dt} + (I_3 - I_2)\omega_y\omega_z = mgl \sin \theta \sin \phi \quad (2.2)$$

$$I_2 \frac{d\omega_y}{dt} + (I_1 - I_3)\omega_x\omega_z = mgl \sin \theta \cos \phi \quad (2.3)$$

$$I_3 \frac{d\omega_z}{dt} + (I_2 - I_1)\omega_x\omega_y = 0 \quad (2.4)$$

We solve Euler's equation for symmetric bodies, i.e., for $I_1 = I_2 = I$. Thus, we see from equation (2.4) that ω_z remains constant. Substituting angular velocity from (2.1)in (2.2) and (2.3),

$$\begin{aligned} \ddot{\theta} \sin \phi + \dot{\theta} \dot{\phi} \cos \phi - \ddot{\psi} \sin \theta \cos \phi - \dot{\psi} \dot{\theta} \cos \theta \cos \phi \\ + \dot{\psi} \dot{\phi} \sin \theta \sin \phi + \omega_z \left(\frac{I_3}{I} - 1 \right) (\dot{\theta} \cos \phi + \dot{\psi} \sin \theta \sin \phi) &= \frac{mgl \sin \theta \sin \phi}{I} \end{aligned} \quad (2.5)$$

$$\begin{aligned} \ddot{\theta} \cos \phi - \dot{\theta} \dot{\phi} \sin \phi + \ddot{\psi} \sin \theta \sin \phi + \dot{\psi} \dot{\theta} \cos \theta \sin \phi \\ + \dot{\psi} \dot{\phi} \sin \theta \cos \phi - \omega_z \left(\frac{I_3}{I} - 1 \right) (\dot{\theta} \sin \phi - \dot{\psi} \sin \theta \cos \phi) &= \frac{mgl \sin \theta \cos \phi}{I} \end{aligned} \quad (2.6)$$

(2.5) $\times \sin \phi +$ (2.6) $\times \cos \phi$ gives,

$$\ddot{\theta} = \frac{mgl \sin \theta}{I} - \dot{\psi} \dot{\phi} \sin \theta - \left(\frac{I_3}{I} - 1 \right) \dot{\psi} \sin \theta. \quad (2.7)$$

And (2.5) $\times \cos \phi -$ (2.6) $\times \sin \phi$ gives,

$$\ddot{\psi} = \frac{I(\dot{\theta} \dot{\phi} - \dot{\psi} \dot{\theta} \cos \theta) + (I_3 - I)\dot{\theta}}{I \sin \theta}. \quad (2.8)$$

Second order differential equations are reduced to first order by introducing variables $\dot{\theta} = n_1$, $\dot{\psi} = n_2$ and $\dot{\phi} = n_3$. Six first order ODEs to be solved are,

$$\begin{aligned} \dot{n}_1 &= \frac{mgl \sin \theta}{I} - n_2(\omega_z - n_2 \cos \theta) \sin \theta - \left(\frac{I_3}{I} - 1 \right) n_2 \sin \theta \\ \dot{n}_2 &= \frac{In_1(\omega_z - 2n_2 \cos \theta) + (I_3 - I)n_1}{I \sin \theta} \\ \dot{n}_3 &= n_1 n_2 \sin \theta \\ \dot{\theta} &= n_1 \\ \dot{\psi} &= n_2 \\ \dot{\phi} &= \omega_z - n_2 \cos \theta \end{aligned}$$

Equations above are solved using Gauss method of order 6 for following initial conditions

$$\begin{array}{ll} \text{mass} = 1.5kg & l = 1.33m \\ \text{step size } h = .005 & \text{tolerance} = 10^{-10} \\ \theta = 45^\circ & \dot{\theta} = 1/s^{-1} \\ \psi = 1^\circ & \dot{\psi} = 1/s^{-1} \\ \phi = 1^\circ & \dot{\phi} = 100/s^{-1} \end{array}$$

Figure 2.13 represents motion of center of mass of the symmetric top as function of time t. Projection of this motion in xy plane in the figure 2.14 shows oscillatory behavior of the motion of the top.

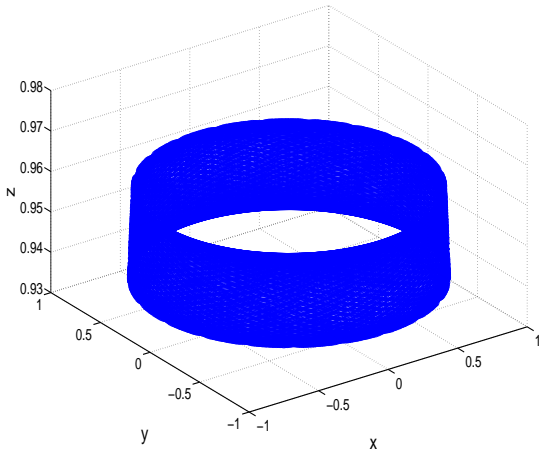


FIGURE 2.13: 3D coordinate of centre of mass

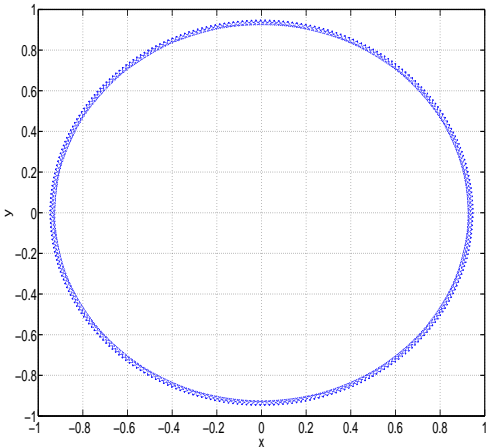


FIGURE 2.14: X-Y coordinate of centre of mass

Some quaternion based, certain properties conserving algorithms have been developed, e.g., energy-angular momentum conserving scheme *QUAT-EM* has been proposed due to Betsch et.al,2009 [12]. Without going into detail of the equations, we show here plots for the motion of symmetric top under gravity for *QUAT-EM* scheme.

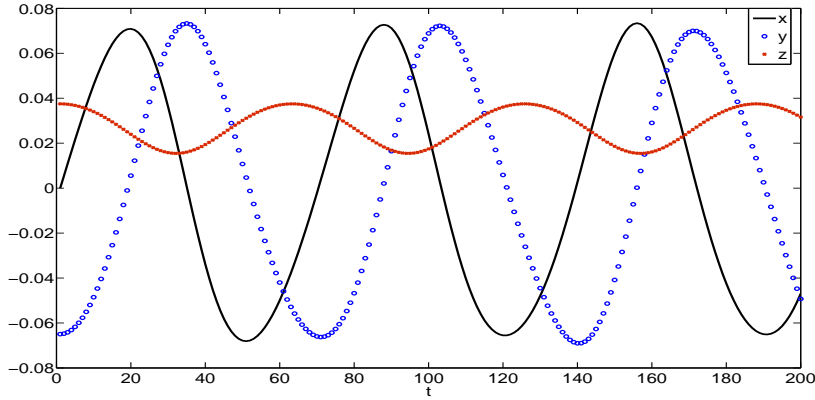


FIGURE 2.15: Coordinates of center of mass of top vs time(in sec.)

Figure 2.15 shows the center of mass coordinates of symmetric top as function of time. Similar to the figure 2.14, periodic behavior of the motion is clear from the plot here.

J_1 , J_2 and J_3 in the figure 2.16 represent angular momentum of the symmetric top in x , y and z directions respectively. As concluded from equation 2.4, J_3 should remain constant. Figure 2.16 clearly shows the conservation of angular momentum J_3 . Figure 2.17 depicts that *QUAT-EM* algorithm successfully conserve the Hamiltonian.

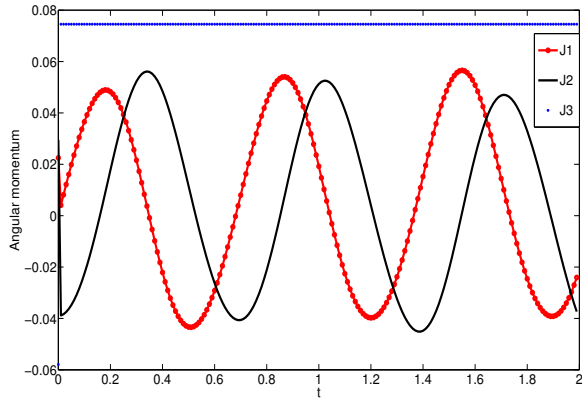


FIGURE 2.16: Angular momentum (in kgm^2s^{-1}) vs time(in sec.)

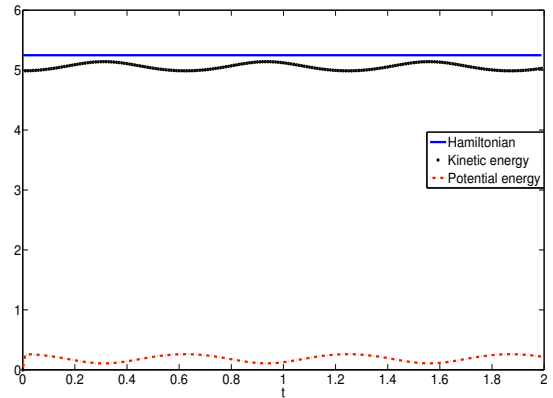


FIGURE 2.17: Hamiltonian of the top(in J) vs time (in sec.)

A rotation matrix based energy conserving *Rattle* algorithm (second order, symplectic) was proposed due to Leimkuhler, pg.207 [7]. Algorithm as been discussed in detail in Appendix B. We reproduce here plots for symmetric plot discussed in Leimkuhler, pg.210 [7]. Figure 2.18 represent z coordinate of center of mass of the symmetric top. Figure 2.19 shows error in the Hamiltonian of the system which is quite small.

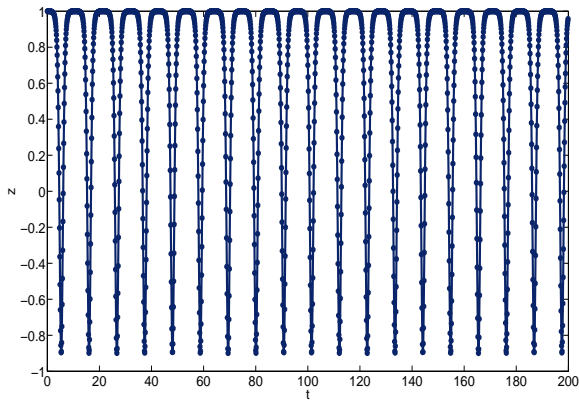


FIGURE 2.18: z coordinate of com

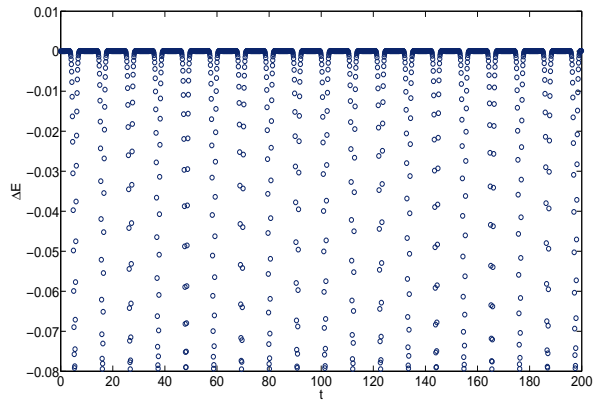


FIGURE 2.19: Error in Hamiltonian

Chapter 3

Dynamics of three dimensional chain

In this chapter, we study the motion of a chain consisting of rigid bodies of arbitrary shape in three dimensional space. In the section 3.2, we represent rotation of the rigid bodies using rotation matrix. In this representation, we solve the system of equations using second order symplectic *Rattle* algorithm (see Appendix B). In the section 3.3, we represent rotation of the rigid bodies using quaternions. We derive the rotational mass matrix in subsection 3.3.1 and prove that it is unique. We incorporate unit quaternion constraint in the Hamiltonian and derive the expression for Lagrangian multiplier in subsection 3.3.8. We show in the section 3.4 that standard symplectic algorithms remain symplectic even after addition of expression for unit quaternion constraint in the Hamiltonian.

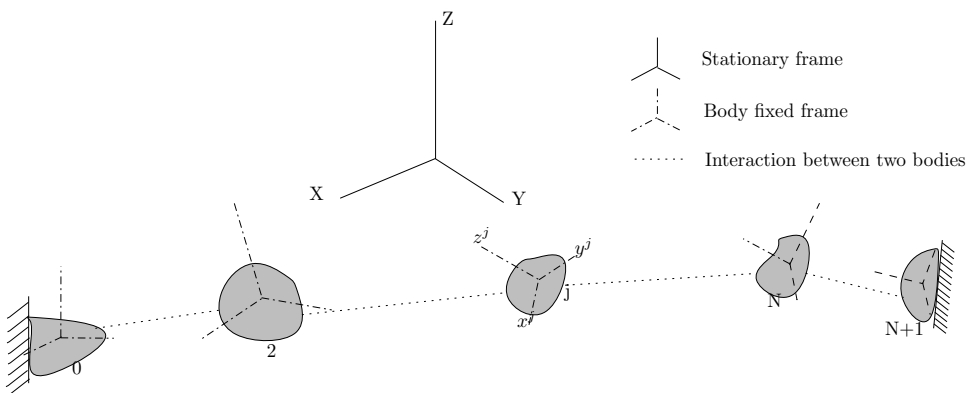


FIGURE 3.1: three dimensional chain of rigid bodies

In the figure 3.1, we represent schematic of the three dimensional chain consisting of $(N+2)$ rigid bodies. Indexing of the bodies start from 0 to $N+1$. In the schematic, boundary condition is clamped-clamped, but we solve the chain problem for more realistic boundary conditions discussed in section 3.3.7.

We assume that rigid bodies are made up of certain number of particles attached to each other through rigid links. In the next section, we derive the moment of inertia of such rigid bodies along its principal axes.

3.1 Rigid body

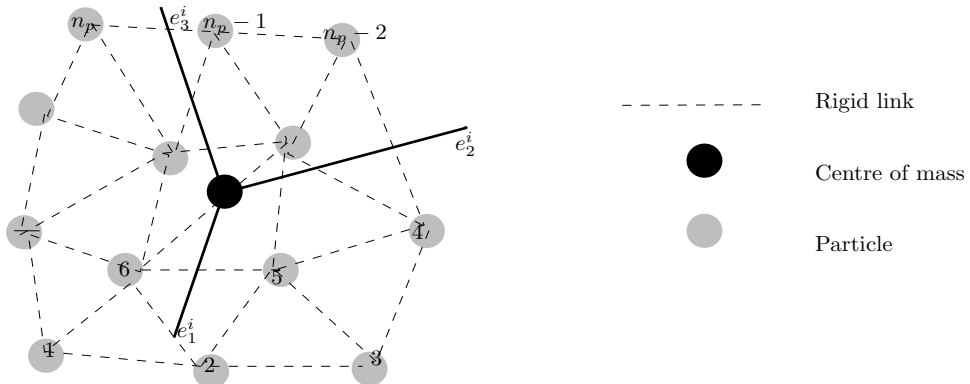


FIGURE 3.2: Configuration of particles in a rigid body

It is assumed that rigid body consist of n_p number of particle attached to each other through rigid links. Let \mathbf{r}_i^k and m_i^k denote the position vector in coordinate frame $\{e_i\}$ and mass of k^{th} particle of i^{th} body respectively. Our aim is to find body fixed coordinate frame with axes at principal axis. We also find position of k^{th} particle with respect to this body fixed frame.

Let \mathbf{r}_i and m_j denote center of mass of i^{th} body in $\{e_i\}$ frame.

$$\mathbf{r}_i = \frac{\sum_{k=1}^{n_p} m_i^k \mathbf{r}_i^k}{\sum_{k=1}^{n_p} m_i^k} = \frac{\sum_{k=1}^{n_p} m_i^k \mathbf{r}_i^k}{m_j}.$$

For now, we consider a body fixed frame with origin at center of mass of the body and having same orientation as frame $\{e_i\}$. In this body fixed frame, component of inertia matrix are,

$$\begin{aligned} I_{11} &= \sum_{k=1}^{n_p} m_i^k \{[(\mathbf{r}_i^k - \mathbf{r}_i) \cdot e_2]^2 + [(\mathbf{r}_i^k - \mathbf{r}_i) \cdot e_3]^2\}, \\ I_{22} &= \sum_{k=1}^{n_p} m_i^k \{[(\mathbf{r}_i^k - \mathbf{r}_i) \cdot e_1]^2 + [(\mathbf{r}_i^k - \mathbf{r}_i) \cdot e_3]^2\}, \\ I_{33} &= \sum_{k=1}^{n_p} m_i^k \{[(\mathbf{r}_i^k - \mathbf{r}_i) \cdot e_1]^2 + [(\mathbf{r}_i^k - \mathbf{r}_i) \cdot e_2]^2\}, \\ I_{12} &= - \sum_{k=1}^{n_p} m_i^k \{[(\mathbf{r}_i^k - \mathbf{r}_i) \cdot e_1][(\mathbf{r}_i^k - \mathbf{r}_i) \cdot e_2]\}, \\ I_{13} &= - \sum_{k=1}^{n_p} m_i^k \{[(\mathbf{r}_i^k - \mathbf{r}_i) \cdot e_1][(\mathbf{r}_i^k - \mathbf{r}_i) \cdot e_3]\}, \\ I_{23} &= - \sum_{k=1}^{n_p} m_i^k \{[(\mathbf{r}_i^k - \mathbf{r}_i) \cdot e_2][(\mathbf{r}_i^k - \mathbf{r}_i) \cdot e_3]\}. \end{aligned}$$

Principal directions Because moment of inertia tensor is a symmetric matrix, it is always possible to diagonalize this matrix.

We relocate position of each particle of the body in the principal coordinate frame (determined from the procedure above). In order to avoid introducing new notation, from now onwards, \mathbf{r}_i^k denote position of k^{th} particle of i^{th} body in principal coordinate frame.

We now study the dynamics of three dimensional chain using rotation matrix scheme in which rotation of rigid bodies are represented using 3×3 rotation matrices.

3.2 Hamiltonian formulation using rotation matrix

Let $\{e_i^j\}_{i=1,2,3}$ denote basis of body fixed frame of j^{th} body. Let $\{e_i\}_{i=1,2,3}$ be the basis of inertial frame. We assume that each rigid body consist of n_p number of particles linked to each other through massless rigid links. Let \mathbf{r}_i^k denote the coordinate of k^{th} particle of j^{th} body in body fixed frame with origin at center of mass. Let \mathbf{r}_j denote the position vector of

center of mass of j^{th} body in stationary frame. Let $\mathbf{R}_j(t) \in SO(3)$ be the rotation matrix relating basis $\{e_i^j\}$ to $\{e_i\}$ as,

$$\{e_i^j\} = \mathbf{R}_j(t)\{e_i\}.$$

Dynamics of the chain is completely determined by position of center of mass of rigid bodies

$$\mathbf{r}_j : \mathbb{R} \rightarrow \mathbb{R}^3, \quad t \mapsto \mathbf{r}_j(t),$$

and orientation of rigid bodies

$$\mathbf{R}_j : \mathbb{R} \rightarrow SO(3), \quad t \mapsto \mathbf{R}_j(t),$$

where, $j = 0, 1, 2, \dots, N + 1$.

So, the configuration space of the system is:

$$\mathcal{C} = \{\mathbb{R}^3 \times \mathbb{R}^3 \dots N+2 \text{ times} \times SO(3) \times SO(3) \dots N+2 \text{ times}\}.$$

In order to write Hamiltonian of the system, we derive expression for total kinetic energy and total potential energy of the system. Let m_j denote the mass of j^{th} rigid body and $[J]^j$ denote principal moment of inertia matrix. Velocity of k^{th} particle of j^{th} body in inertial frame is,

$$\dot{\mathbf{r}}_j + \dot{\mathbf{R}}_j^T(t)\mathbf{r}_j^k.$$

Therefore, kinetic energy of j^{th} body is ,

$$T^j = \frac{1}{2} \sum_{k=1}^{n_p} m_j \|\dot{\mathbf{r}}_j\|^2 + \frac{1}{2} \operatorname{tr} \left(\dot{\mathbf{R}}_j^T(t) [J]^j \dot{\mathbf{R}}_j(t) \right).$$

In expression above, the first term represent translational kinetic energy of the body, T_{trans}^j and second term denotes rotational kinetic energy, T_{rot}^j .

Let the interaction potential be depending on relative distance between two bodies and their relative orientation. Let us assume nearest neighbor interaction. Then, the general form of potential energy contribution from the pair, i^{th} and j^{th} body is

$$V_{ij} = V_{ij}(\mathbf{R}_i, \mathbf{R}_j, \mathbf{r}_i, \mathbf{r}_j). \quad (3.1)$$

So, Lagrangian of the system is,

$$\mathcal{L} = \sum_{j=0}^{N+1} \{T_{rot}^j(\dot{\mathbf{R}}_j(t)) + T_{trans}^j(\dot{\mathbf{r}}_j)\} - \sum_{j=0}^N V_{j,j+1}(\mathbf{R}_j, \mathbf{R}_{j+1}, \mathbf{r}_j, \mathbf{r}_{j+1}). \quad (3.2)$$

Using Legendre transformation, conjugate rotational momenta \mathbf{P}_j and translational momenta \mathbf{p}_j are calculated as,

$$\mathbf{P}_j = \frac{\partial \mathcal{L}}{\partial \dot{\mathbf{R}}_j} = \dot{\mathbf{R}}_j[J]^j, \quad (3.3)$$

$$\mathbf{p}_j = \frac{\partial \mathcal{L}}{\partial \dot{\mathbf{r}}_j} = m_j \dot{\mathbf{r}}_j. \quad (3.4)$$

Kinetic energy of the system in terms of conjugate momenta is,

$$\sum_{j=0}^{N+1} \left\{ \frac{1}{2} \text{tr} (\mathbf{P}_j [J]^{-1} \mathbf{P}_j^T) + \frac{\|\mathbf{p}_j\|^2}{2m_j} \right\}. \quad (3.5)$$

Hamiltonian of the system is given by

$$\mathcal{H} = \sum_{j=0}^{N+1} \left\{ \frac{1}{2} \text{tr} (\mathbf{P}_j [J]^{-1} \mathbf{P}_j^T) + \frac{\|\mathbf{p}_j\|^2}{2m_j} \right\} + \sum_{j=0}^N V_{j,j+1}(\mathbf{R}_j, \mathbf{R}_{j+1}, \mathbf{r}_j, \mathbf{r}_{j+1}).$$

3.2.1 Constraints

Leimkuhler and Reich [7] and Betsch et. al.,[8] have discussed the constraints to be put on the rotation matrix $\mathbf{R}_j(t)$ and the conjugate momenta $\mathbf{P}_j(t)$. Matrix $\mathbf{R}_j(t)$ represent rotation matrix iff it satisfy the orthogonality condition

$$\mathbf{R}_j \mathbf{R}_j^T = I_{3 \times 3} \quad \text{and} \quad \mathbf{R}_j^T \mathbf{R}_j = I_{3 \times 3}.$$

Because $\mathbf{R}_j \mathbf{R}_j^T$ is a symmetric matrix, there are six independent constraints on $\mathbf{R}_j(t)$. This should be expected as we are using 9 variables (3×3 matrix) to represent the rotation in \mathbb{R}^3 .

In order to enforce orthogonality condition constraint, Leimkuhler and Reich [7] introduced

six Lagrange multipliers through a symmetric matrix Λ^j . So, Hamiltonian of the system is modified by adding the term

$$\sum_{j=0}^{N+1} \text{tr}\{(\mathbf{R}_j \mathbf{R}_j^T - I) \Lambda^j\}. \quad (3.6)$$

Constraint on conjugate momenta is obtained by differentiating above equation with respect to time and using (3.4),

$$\mathbf{R}_j^T \mathbf{P}_j [J]^{j-1} + [J]^{j-1} \mathbf{P}_j^T \mathbf{R}_j = 0. \quad (3.7)$$

3.2.2 Hamilton's equations

Hamiltonian of the system, after adding the term 3.6 is,

$$\mathcal{H} = \sum_{j=0}^{N+1} \left\{ \frac{1}{2} \text{tr} (\mathbf{P}_j [J]^{-1} \mathbf{P}_j^T) + \frac{\|\mathbf{p}_j\|^2}{2m_j} \right\} + \sum_{j=0}^N V_{j,j+1}(\mathbf{R}_j, \mathbf{R}_{j+1}, \mathbf{r}_j, \mathbf{r}_{j+1}) + \sum_{j=0}^{N+1} \text{tr}\{(\mathbf{R}_j \mathbf{R}_j^T - I) \Lambda^j\}. \quad (3.8)$$

Phase space of this Hamiltonian system is:

$$\mathcal{P} = \{(\mathbf{r}_j, \mathbf{p}_j, \mathbf{R}_j, \mathbf{P}_j)_{j=0,1,\dots,N+1} \in \mathcal{M} : \mathbf{R}_j^T \mathbf{R}_j = I_3, \mathbf{R}_j^T \mathbf{P}_j [J]^{j-1} + [J]^{j-1} \mathbf{P}_j^T \mathbf{R}_j = 0\},$$

where,

$$\mathcal{M} = \{\mathbb{R}^3 \times \mathbb{R}^3 \dots 2N+4 \text{ times} \times SO(3) \times SO(3) \dots 2N+4 \text{ times}\}.$$

Using Hamilton's equations,

$$\frac{d\mathbf{P}_j}{dt} = -\frac{\partial \mathcal{H}}{\partial \mathbf{R}_j}, \quad \frac{d\mathbf{R}_j}{dt} = \frac{\partial \mathcal{H}}{\partial \mathbf{P}_j}, \quad \frac{d\mathbf{p}_j}{dt} = -\frac{\partial \mathcal{H}}{\partial \mathbf{r}_j}, \quad \frac{d\mathbf{r}_j}{dt} = \frac{\partial \mathcal{H}}{\partial \mathbf{p}_j}. \quad (3.9)$$

Therefore, Hamilton's equations on phase space \mathcal{P} are,

$$\frac{d\mathbf{p}_j}{dt} = -\frac{\partial}{\partial \mathbf{r}_j} (V_{j-1,j} + V_{j,j+1}), \quad (3.10a)$$

$$\frac{d\mathbf{r}_j}{dt} = \frac{\mathbf{p}_j}{m_j}, \quad (3.10b)$$

$$\frac{d\mathbf{P}_j}{dt} = -\frac{\partial}{\partial \mathbf{R}_j} (V_{j-1,j} + V_{j,j+1}) - 2\mathbf{R}_j \Lambda^j, \quad (3.10c)$$

$$\frac{d\mathbf{R}_j}{dt} = \mathbf{P}_j [J]^{j-1}. \quad (3.10d)$$

Above equations are valid for $j = 1$ to $j = N$. Equations for 0^{th} and $(N + 1)^{th}$ body are taken care of in boundary conditions.

3.2.3 Gradient of Potential

In this subsection, we derive the gradient of potential with respect to rotation matrix \mathbf{R}_j and with respect to position vector \mathbf{r}_j . We assume, the interaction to be of particle-particle type. In that case potential energy contribution from k^{th} particle of i^{th} body and l^{th} particle of j^{th} body is the function of distance $r_{i,j}^{k,l}$ between them, given by

$$\begin{aligned} \{r_{i,j}^{k,l}\}^2 &= \{(\mathbf{r}_i + \mathbf{R}_i^T \mathbf{r}_i^k) - (\mathbf{r}_j + \mathbf{R}_j^T \mathbf{r}_j^l)\} \cdot \{(\mathbf{r}_i + \mathbf{R}_i^T \mathbf{r}_i^k) - (\mathbf{r}_j + \mathbf{R}_j^T \mathbf{r}_j^l)\} \\ &= \mathbf{r}_i \cdot \mathbf{r}_i + 2\mathbf{r}_i \cdot \mathbf{R}_i^T \mathbf{r}_i^k + \mathbf{r}_i^k \cdot \mathbf{r}_i^k + \mathbf{r}_j \cdot \mathbf{r}_j + 2\mathbf{r}_j \cdot \mathbf{R}_j^T \mathbf{r}_j^l + \mathbf{r}_j^l \cdot \mathbf{r}_j^l \\ &\quad - 2(\mathbf{r}_i \cdot \mathbf{r}_j + \mathbf{r}_i \cdot \mathbf{R}_j^T \mathbf{r}_j^l + \mathbf{r}_j \cdot \mathbf{R}_i^T \mathbf{r}_i^k + \mathbf{R}_i^T \mathbf{r}_i^k \cdot \mathbf{R}_j^T \mathbf{r}_j^l). \end{aligned} \quad (3.11)$$

So, the contribution to potential energy from the pair i^{th} and j^{th} body is given by

$$V_{ij} = \sum_{k=1}^{n_p} \sum_{l=1}^{n_p} V_{ij}^{k,l}(r_{i,j}^{k,l}). \quad (3.12)$$

Using above equation and chain rule, we rewrite Hamilton's equations (3.13a)-(3.13d) on phase space \mathcal{P} in terms of the potential gradients as

$$\begin{aligned} \frac{d\mathbf{p}_j}{dt} &= - \sum_{k=1}^{n_p} \sum_{l=1}^{n_p} A_{j-1,j}^{k,l} \{\mathbf{r}_j + \mathbf{R}_j^T \mathbf{r}_j^l - \mathbf{r}_{j-1} - \mathbf{R}_{j-1}^T \mathbf{r}_{j-1}^k\} \\ &\quad + A_{j,j+1}^{k,l} \{\mathbf{r}_j + \mathbf{R}_j^T \mathbf{r}_j^k - \mathbf{r}_{j+1} - \mathbf{R}_{j+1}^T \mathbf{r}_{j+1}^l\}, \end{aligned} \quad (3.13a)$$

$$\frac{d\mathbf{r}_j}{dt} = \frac{\mathbf{p}_j}{m_j}, \quad (3.13b)$$

$$\begin{aligned} \frac{d\mathbf{P}_j}{dt} &= - \sum_{k=1}^{n_p} \sum_{l=1}^{n_p} A_{j-1,j}^{k,l} \mathbf{r}_j^l \{\mathbf{r}_j^T - \mathbf{r}_{j-1}^T - \mathbf{r}_{j-1}^{kT} \mathbf{R}_{j-1}\} \\ &\quad + A_{j,j+1}^{k,l} \mathbf{r}_j^k \{\mathbf{r}_j^T - \mathbf{r}_{j+1}^T - \mathbf{r}_{j+1}^{lT} \mathbf{R}_{j+1}\} - 2\mathbf{R}_j \Lambda^j, \end{aligned} \quad (3.13c)$$

$$\frac{d\mathbf{R}_j}{dt} = \mathbf{P}_j [J]^{j-1}, \quad (3.13d)$$

where,

$$A_{p,q}^{k,l} = \frac{\partial V_{p,q}^{k,l}}{\partial r_{p,q}^{k,l}} \frac{1}{r_{p,q}^{k,l}}.$$

3.2.4 Boundary condition

We consider 3 possible set of boundary conditions, $c_1 - c_1$, $c_1 - c_2$ and $c_1 - c_3$, which have been described below.

1. $c_1 - c_1$: In this case, both ends are clamped. Hence, coordinates of 0^{th} and $(N + 1)^{th}$ body remain same for all time.

$$\begin{aligned} \mathbf{r}_0(t) &= \mathbf{r}_0(0), & \mathbf{R}_0(t) &= \mathbf{R}_0(0), \\ \mathbf{r}_{N+1}(t) &= \mathbf{r}_{N+1}(0), & \mathbf{R}_{N+1}(t) &= \mathbf{R}_{N+1}(0), \\ \mathbf{p}_0(t) &= 0_{3 \times 1}, & \mathbf{P}_0(t) &= 0_{3 \times 3}, \\ \mathbf{p}_{N+1}(t) &= 0_{3 \times 1}, & \mathbf{P}_{N+1}(t) &= 0_{3 \times 3}. \end{aligned}$$

Equations (3.13a)-(3.13d) are solved for $j = 1, 2, 3, \dots, N$.

2. $c_1 - c_2$: In this case, one end is clamped and force is applied at other end, but this end is free to rotate. So, for 0^{th} body,

$$\begin{aligned} \mathbf{r}_0(t) &= \mathbf{r}_0(0), & \mathbf{R}_0(t) &= \mathbf{R}_0(0), \\ \mathbf{p}_0(t) &= 0_{3 \times 1}, & \mathbf{P}_0(t) &= 0_{3 \times 3}. \end{aligned}$$

Let the applied constant force be \mathbf{F} . Then work done on the system is,

$$\mathcal{W}_F = -\mathbf{F} \cdot \mathbf{r}_{N+1}.$$

We add this work \mathcal{W}_F to the Hamiltonian of the system (3.8) and using Hamilton's equations (3.13a)-(3.13d), we get equations for $(N + 1)^{th}$ body as,

$$\begin{aligned}\frac{d\mathbf{p}_{N+1}}{dt} &= - \sum_{k=1}^{n_p} \sum_{l=1}^{n_p} A_{N,N+1}^{k,l} \{ \mathbf{r}_{N+1} + \mathbf{R}_{N+1}^T \mathbf{r}_{N+1}^l - \mathbf{r}_N - \mathbf{R}_N^T \mathbf{r}_N^k \} + \mathbf{F}, \\ \frac{d\mathbf{r}_{N+1}}{dt} &= \frac{\mathbf{p}_{N+1}}{m_{N+1}}, \\ \frac{d\mathbf{P}_{N+1}}{dt} &= - \sum_{k=1}^{n_p} \sum_{l=1}^{n_p} A_{N,N+1}^{k,l} \mathbf{r}_{N+1}^l \{ \mathbf{r}_{N+1}^T - \mathbf{r}_N^T - \mathbf{r}_N^{kT} \mathbf{R}_N \} - 2\mathbf{R}_{N+1} \Lambda^{N+1}, \\ \frac{d\mathbf{R}_{N+1}}{dt} &= \mathbf{P}_{N+1} [J]^{N+1-1}.\end{aligned}$$

Equations for $j = 1, 2, \dots, N$ remain same as in (3.13a)-(3.13d).

3. $c_1 - c_3$: In this case, one end is clamped and constant displacement \mathbf{d} is specified at other end, but this end is free to rotate. So, the boundary conditions are

$$\begin{aligned}\mathbf{r}_0(t) &= \mathbf{r}_0(0), & \mathbf{R}_0(t) &= \mathbf{R}_0(0), \\ \mathbf{p}_0(t) &= 0_{3 \times 1}, & \mathbf{P}_0(t) &= 0_{3 \times 3}, \\ \mathbf{r}_{N+1}(t) &= \mathbf{d}, & \mathbf{p}_{N+1}(t) &= 0_{3 \times 1}.\end{aligned}$$

Because the position of $(N + 1)^{th}$ body is given as constant displacement \mathbf{d} , $\dot{\mathbf{r}}_{N+1} = 0$ and $\dot{\mathbf{p}}_{N+1} = 0$. Therefore, using (3.13a)-(3.13d), equations for $(N + 1)^{th}$ body are

$$\begin{aligned}\frac{d\mathbf{p}_{N+1}}{dt} &= 0_{3 \times 1}, \\ \frac{d\mathbf{r}_{N+1}}{dt} &= 0_{3 \times 1}, \\ \frac{d\mathbf{P}_{N+1}}{dt} &= - \sum_{k=1}^{n_p} \sum_{l=1}^{n_p} A_{N,N+1}^{k,l} \mathbf{r}_{N+1}^l \{ \mathbf{d}^T - \mathbf{r}_N^T - \mathbf{r}_N^{kT} \mathbf{R}_N \} - 2\mathbf{R}_{N+1} \Lambda^{N+1}, \\ \frac{d\mathbf{R}_{N+1}}{dt} &= \mathbf{P}_{N+1} [J]^{N+1-1}.\end{aligned}$$

Equations for $j = 1, 2, \dots, N$ remain same as in (3.13a)-(3.13d).

Rotation matrix based symplectic schemes have been proposed due to Leimkuhler and Sebastian [7]. We have extended this idea to multibody problem and have proposed Hamiltonian formulation for three dimensional chain. Numerical schemes base on rotation matrix have been proposed due to Leimkuhler [7] and Shuichi[23]. Appendix B discuss Rattle [7] algorithm in detail. Because this representation has larger configuration space than quaternion representation, we will be using quaternion based schemes to solve the system numerically. However, rotation matrix scheme is still better than Euler's angle scheme as it does not involve any singularity and hence should be given preference over Euler's angle scheme.

As discussed earlier, quaternion schemes have advantage over rotation matrix scheme because of lesser dimensional configuration space. We develop a quaternion based scheme for studying dynamics of three dimensional chain.

3.3 Hamiltonian formulation using quaternion

Let $\{e_i^j\}_{i=1,2,3}$ denote basis of body fixed frame of j^{th} body. Let $\{e_i\}_{i=1,2,3}$ be the basis of inertial frame. Let \mathbf{r}_j denote the position vector of center of mass of j^{th} body in stationary frame. Motion of three dimensional chain consisting of $(N + 2)$ number of rigid bodies is completely determined by coordinate of center of mass of rigid bodies

$$\mathbf{r}_j : \mathbb{R} \rightarrow \mathbb{R}^3, \quad t \mapsto \mathbf{r}_j(t),$$

and set of unit quaternions

$$\mathbf{q}_j : \mathbb{R} \rightarrow \mathbb{S}^3 = \partial B_1^{\mathbb{H}}(0) \hookrightarrow \mathbb{H}, \quad t \mapsto \mathbf{q}_j(t),$$

where, $j = 0, 1, 2, \dots, N + 2$, and the set of unit quaternions $\mathbb{S}^3 = \partial B_1^{\mathbb{H}}(0) = \{\mathbf{q}_j \in \mathbb{H} : \|\mathbf{q}\| = 1\} \subset \mathbb{H}$, is a subgroup of the multiplicative quaternion group \mathbb{H} .

Configuration space of the system is:

$$\mathcal{C} = \{\mathbb{R}^3 \times \mathbb{R}^3 \dots N+2 \text{ times} \times \mathbb{H} \times \mathbb{H} \dots N+2 \text{ times}\}.$$

For the quaternion $\mathbf{q}_j = \{q_{j,0}, q_{j,1}, q_{j,2}, q_{j,3}\}^T \in \{\mathbb{R}^4 = \mathbb{H}\}$, rotation matrix $\mathbf{R}(\mathbf{q}_j)$ is given by Euler map

$$\mathbf{R} : \mathbb{H} \rightarrow SO(3), \quad \mathbf{q}_j \rightarrow \mathbf{R}(\mathbf{q}_j),$$

where,

$$R(\mathbf{q}_j) = \begin{bmatrix} 2q_{j,0}^2 + 2q_{j,1}^2 - 1 & 2q_{j,1}q_{j,2} - 2q_{j,0}q_{j,3} & 2q_{j,1}q_{j,3} + 2q_{j,0}q_{j,2} \\ 2q_{j,1}q_{j,2} + 2q_{j,0}q_{j,3} & 2q_{j,0}^2 + 2q_{j,2}^2 - 1 & 2q_{j,2}q_{j,3} - 2q_{j,0}q_{j,1} \\ 2q_{j,3}q_{j,1} - 2q_{j,0}q_{j,2} & 2q_{j,3}q_{j,2} + 2q_{j,0}q_{j,1} & 2q_{j,0}^2 + 2q_{j,3}^2 - 1 \end{bmatrix}. \quad (3.14)$$

We have derived this Euler map in Appendix A.

In order to write Hamiltonian of the system, we derive total kinetic energy and total potential energy of the system in terms of quaternions. Translational kinetic energy is independent of quaternion and is given by

$$T_{trans}^j = \frac{\mathbf{p}_j^2}{2m_j}, \quad (3.15)$$

where, \mathbf{p}_j and m_j are linear momentum and mass of j^{th} body respectively.

We have derived angular velocity of a rotating body in terms of quaternions in Appendix A. Angular velocity ω^j of j^{th} body depends on both, the quaternion \mathbf{q}_j and its time derivative $\dot{\mathbf{q}}_j$. Therefore, rotational mass matrix, unlike translational mass matrix, will not be a constant and hence need special mention.

3.3.1 Rotational mass matrix

Rotation kinetic energy of j^{th} rigid body is given by

$$T_{rot}^j = \frac{1}{2}\omega^j{}^T [J]^j \omega^j,$$

where ω^j is the angular velocity of the j^{th} body in body fixed frame and $[J]^j$ is the principal moment of inertia matrix. Angular velocity ω^j from (A.12) is

$$\omega^j = 2G(\mathbf{q}_j)\dot{\mathbf{q}}_j, \quad G(\mathbf{q}_j) = \begin{bmatrix} -q_{j,1} & q_{j,0} & q_{j,3} & -q_{j,2} \\ -q_{j,2} & -q_{j,3} & q_{j,0} & q_{j,1} \\ -q_{j,3} & q_{j,2} & -q_{j,1} & q_{j,0} \end{bmatrix}.$$

Substituting ω^j in kinetic energy,

$$T_{rot}^j = 2\dot{\mathbf{q}}_j^T G(\mathbf{q}_j)^T [J]^j G(\mathbf{q}_j) \dot{\mathbf{q}}_j.$$

Using Legendre transformation, conjugate momenta \mathbf{g}_j is given by

$$\begin{aligned} \mathbf{g}_j &= \frac{\partial T_{rot}^j}{\partial \dot{\mathbf{q}}_j} \\ &= 4G(\mathbf{q}_j)^T [J]^j G(\mathbf{q}_j) \dot{\mathbf{q}}_j. \end{aligned}$$

From the construction of $G(\mathbf{q}_j)$, we see that $G(\mathbf{q}_j)\mathbf{q}_j = 0$. Thus there is rank deficiency in the matrix $G(\mathbf{q}_j)^T [J]^j G(\mathbf{q}_j)$ and hence, is non-invertible. Therefore, we cannot get $\dot{\mathbf{q}}_j$ in terms of \mathbf{g}_j .

Lemma 1. In order to get $\dot{\mathbf{q}}_j$ in terms of \mathbf{g}_j , augmented matrices $\hat{\omega}(\mathbf{q}_j, \dot{\mathbf{q}}_j)$, $\hat{G}(\mathbf{q}_j)$ and $[\hat{J}]^j$ are introduced such that

$$\hat{\omega}(\mathbf{q}_j, \dot{\mathbf{q}}_j) = [0 \ \omega^T]^T = 2\hat{G}(\mathbf{q}_j)_{4 \times 4}[\dot{\mathbf{q}}_j],$$

$$\hat{G}(\mathbf{q}_j) = \begin{bmatrix} q_{j,0} & q_{j,1} & q_{j,2} & q_{j,3} \\ -q_{j,1} & q_{j,0} & q_{j,3} & -q_{j,2} \\ -q_{j,2} & -q_{j,3} & q_{j,0} & q_{j,1} \\ -q_{j,3} & q_{j,2} & -q_{j,1} & q_{j,0} \end{bmatrix}, \quad (3.16)$$

and

$$[\hat{J}]^j = \begin{bmatrix} 1 & 0 & 0 & 0 \\ 0 & J_1^j & 0 & 0 \\ 0 & 0 & J_2^j & 0 \\ 0 & 0 & 0 & J_3^j \end{bmatrix}. \quad (3.17)$$

Proof: Appendix C

So, the rotational kinetic energy in terms of augmented matrices is,

$$T_{rot}^j = \frac{1}{2} \dot{\mathbf{q}}_j^T \mu(\mathbf{q}_j) \dot{\mathbf{q}}_j,$$

where,

$$\mu(\mathbf{q}_j) = 4\hat{G}(\mathbf{q}_j)^T [\hat{J}]^j \hat{G}(\mathbf{q}_j). \quad (3.18)$$

denotes the rotational mass matrix.

We have derived the rotational mass matrix which is invertible and have show that it is unique. This mass matrix is the function of quaternion \mathbf{q}_j as expected from the form of angular velocity ω .

Using this invertible mass matrix, we derive the rotational kinetic energy in terms conjugate momenta.

3.3.2 Rotational kinetic energy

From above subsection,

$$T_{rot}^j = \frac{1}{2} \dot{\mathbf{q}}_j^T \mu(\mathbf{q}_j) \dot{\mathbf{q}}_j.$$

We obtain the conjugate momenta by legendre transform,

$$\mathbf{g}_j = \frac{\partial T_{rot}}{\partial \dot{\mathbf{q}}} = \mu(\mathbf{q}_j) \dot{\mathbf{q}}_j.$$

Using $[\hat{G}(\mathbf{q}_j)^{-1} = \hat{G}(\mathbf{q}_j)^T]$,

$$\dot{\mathbf{q}}_j = \mu^{-1}(\mathbf{q}_j) \mathbf{g}_j,$$

where,

$$\mu^{-1}(\mathbf{q}_j) = \frac{1}{4}\hat{G}(\mathbf{q}_j)^T[\hat{J}^j]^{-1}\hat{G}(\mathbf{q}_j). \quad (3.19)$$

So, the rotational kinetic energy in terms of conjugate momenta is

$$T_{rot}^j = \frac{1}{2}\mathbf{g}_j^T\mu^{-1}(\mathbf{q}_j)\mathbf{g}_j.$$

By structure of $\hat{G}(\mathbf{q}_j)$ from equation C.3, we see that

$$\hat{G}(\mathbf{q}_j)\mathbf{g}_j = -\hat{G}(\mathbf{g}_j)\mathbf{q}. \quad (3.20)$$

Hence,

$$T_{rot}^j = \frac{1}{2}\mathbf{g}_j^T\mu^{-1}(\mathbf{q}_j)\mathbf{g}_j = \frac{1}{2}\mathbf{q}_j^T\mu^{-1}(\mathbf{g}_j)\mathbf{q}_j. \quad (3.21)$$

Above equations is useful when we differentiate the Hamiltonian with quaternion \mathbf{q}_j .

3.3.3 Potential energy

Our system consists of $(N+2)$ bodies, indexing from 0 to $N+1$. We assume that j^{th} body interact with its nearest neighbors, i.e., with $(j-1)^{th}$ body and $(j+1)^{th}$ body. It is also assumed that potential energy depends on relative position of center of mass of the bodies and their relative orientation. So, the general form of potential energy of the system is given by

$$V = \sum_{j=0}^N V_{j,j+1}, \quad V_{ij} = V_{ij}(\mathbf{q}_j, \mathbf{q}_{j+1}, \mathbf{r}_j, \mathbf{r}_{j+1}). \quad (3.22)$$

3.3.4 Constraints

Unit quaternion constraint is incorporated in Hamiltonian by adding the term,

$$\sum_{j=1}^N \lambda_j (\mathbf{q}_j^T \mathbf{q}_j - 1), \quad (3.23)$$

where, λ_j is the Lagrangian multiplier corresponding to j^{th} body. Because quaternion (vector in \mathbb{R}^4) represents rotation in \mathbb{R}^3 , there is only one constraint equation. We derive the

constraint on conjugate momenta \mathbf{g}_j

$$\mathbf{q}_j^T \mathbf{g}_j = 0,$$

in the subsection 3.3.8.

We, now have total kinetic energy , total potential energy and constraints on the system. So, we derive the Hamilton's equation for the three dimensional chain in terms of quaternions.

3.3.5 Hamiltonian

Hamiltonian of the system is :

$$\mathcal{H} = \mathcal{H}(\mathbf{p}_1, \dots, \mathbf{p}_n, \mathbf{r}_1, \dots, \mathbf{r}_n, \mathbf{g}_1, \dots, \mathbf{g}_n, \mathbf{q}_1, \dots, \mathbf{q}_n). \quad (3.24)$$

Phase space coordinates $(\mathbf{g}_j, \mathbf{q}_j)_{j=0,1,\dots,N+1}$ lie on the manifold,

$$\mathcal{P} = \{(\mathbf{g}_j, \mathbf{q}_j)_{j=0,1,\dots,N+1} \in \mathbb{H} \times \mathbb{H} \dots 2N+4 \text{ times} : \mathbf{q}_j^T \mathbf{q}_j = 1, \mathbf{q}_j^T \mathbf{g}_j = 0\}. \quad (3.25)$$

We suppress argument of Hamiltonian from now onwards.

$$\mathcal{H} = \sum_{j=0}^{N+1} \frac{1}{2} \mathbf{g}_j^T \mu^{-1}(\mathbf{q}_j) \mathbf{g}_j + \sum_{j=0}^{N+1} \frac{\mathbf{p}_j^2}{2m_j} + \sum_{j=0}^N V_{j,j+1}(\mathbf{q}_j, \mathbf{q}_{j+1}, \mathbf{r}_j, \mathbf{r}_{j+1}) + \sum_{j=0}^{N+1} \lambda_j (\mathbf{q}_j^T \mathbf{q}_j - 1). \quad (3.26)$$

Using Hamilton's equations,

$$\frac{d\mathbf{g}_j}{dt} = -\frac{\partial \mathcal{H}}{\partial \mathbf{q}_j}, \frac{d\mathbf{q}_j}{dt} = \frac{\partial \mathcal{H}}{\partial \mathbf{g}_j}, \frac{d\mathbf{p}_j}{dt} = -\frac{\partial \mathcal{H}}{\partial \mathbf{r}_j}, \frac{d\mathbf{r}_j}{dt} = \frac{\partial \mathcal{H}}{\partial \mathbf{p}_j}. \quad (3.27)$$

Therefore, Hamilton's equations on the phase space \mathcal{P} are

$$\frac{d\mathbf{p}_j}{dt} = -\frac{\partial}{\partial \mathbf{r}_j} \{ V_{j-1,j}(\mathbf{q}_{j-1}, \mathbf{q}_j, \mathbf{r}_{j-1}, \mathbf{r}_j) + V_{j,j+1}(\mathbf{q}_j, \mathbf{q}_{j+1}, \mathbf{r}_j, \mathbf{r}_{j+1}) \}, \quad (3.28a)$$

$$\frac{d\mathbf{r}_j}{dt} = \frac{\mathbf{p}_j}{m_j}, \quad (3.28b)$$

$$\begin{aligned} \frac{d\mathbf{g}_j}{dt} &= -\mu^{-1}(\mathbf{g}_j)\mathbf{q}_j - \frac{\partial}{\partial \mathbf{q}_j} \{ V_{j-1,j}(\mathbf{q}_{j-1}, \mathbf{q}_j, \mathbf{r}_{j-1}, \mathbf{r}_j) \\ &\quad + V_{j,j+1}(\mathbf{q}_j, \mathbf{q}_{j+1}, \mathbf{r}_j, \mathbf{r}_{j+1}) \} - 2\lambda_j \mathbf{q}_j, \end{aligned} \quad (3.28c)$$

$$\frac{d\mathbf{q}_j}{dt} = \mu^{-1}(\mathbf{q}_j)\mathbf{g}_j. \quad (3.28d)$$

Above equations are applicable for $j = 1, 2, \dots, N$. Equations for $j = 0, N + 1$ are given according to boundary conditions.

3.3.6 Gradient of potential

In this subsection, we derive the gradient of potential with respect to rotation matrix $R(\mathbf{q}_i)$ and with respect to position vector \mathbf{r}_i . We assume, the interaction to be of particle-particle type. In that case potential energy contribution from k^{th} particle of i^{th} body and l^{th} particle of j^{th} body is the function of distance $r_{i,j}^{k,l}$ between them, given by

$$\begin{aligned} \{r_{i,j}^{k,l}\}^2 &= \{(\mathbf{r}_i + R(\mathbf{q}_i)^T \mathbf{r}_i^k) - (\mathbf{r}_j + R(\mathbf{q}_j)^T \mathbf{r}_j^l)\} \cdot \{(\mathbf{r}_i + R(\mathbf{q}_i)^T \mathbf{r}_i^k) - (\mathbf{r}_j + R(\mathbf{q}_j)^T \mathbf{r}_j^l)\} \\ &= \mathbf{r}_i \cdot \mathbf{r}_i + 2\mathbf{r}_i \cdot R(\mathbf{q}_i)^T \mathbf{r}_i^k + \mathbf{r}_i^k \cdot \mathbf{r}_i^k + \mathbf{r}_j \cdot \mathbf{r}_j + 2\mathbf{r}_j \cdot R(\mathbf{q}_j)^T \mathbf{r}_j^l + \mathbf{r}_j^l \cdot \mathbf{r}_j^l \\ &\quad - 2(\mathbf{r}_i \cdot \mathbf{r}_j + \mathbf{r}_i \cdot R(\mathbf{q}_j)^T \mathbf{r}_j^l + \mathbf{r}_j \cdot R(\mathbf{q}_i)^T \mathbf{r}_i^k + R(\mathbf{q}_i)^T \mathbf{r}_i^k \cdot R(\mathbf{q}_j)^T \mathbf{r}_j^l). \end{aligned} \quad (3.29)$$

So, the contribution to potential energy from the pair i^{th} and j^{th} body is

$$V_{ij} = \sum_{k=1}^{n_p} \sum_{l=1}^{n_p} V_{ij}^{k,l}(r_{i,j}^{k,l}). \quad (3.30)$$

Therefore,

$$\frac{\partial V_{ij}}{\partial \mathbf{r}_i} = \sum_{k=1}^{n_p} \sum_{l=1}^{n_p} \frac{\partial V_{ij}^{k,l}}{\partial \mathbf{r}_i} = \sum_{k=1}^{n_p} \sum_{l=1}^{n_p} \frac{\partial V_{ij}^{k,l}}{\partial r_{i,j}^{k,l}} \frac{\partial r_{i,j}^{k,l}}{\partial \mathbf{r}_i}.$$

For obtaining the derivative of potential with respect to position vector \mathbf{r}_j , we calculate

$$\frac{\partial r_{i,j}^{k,l}}{\partial \mathbf{r}_i} = \frac{1}{r_{i,j}^{k,l}} \{ \mathbf{r}_i + R(\mathbf{q}_i)^T \mathbf{r}_i^k - (\mathbf{r}_j + R(\mathbf{q}_j)^T \mathbf{r}_j^l) \}.$$

Similarly for differentiation with respect to quaternion \mathbf{q}_i ,

$$\frac{\partial V_{ij}}{\partial \mathbf{q}_i} = \sum_{k=1}^{n_p} \sum_{l=1}^{n_p} \frac{\partial V_{ij}^{k,l}}{\partial \mathbf{q}_i} = \sum_{k=1}^{n_p} \sum_{l=1}^{n_p} \frac{\partial V_{ij}^{k,l}}{\partial r_{i,j}^{k,l}} \frac{\partial r_{i,j}^{k,l}}{\partial \mathbf{q}_i},$$

where,

$$\frac{\partial r_{i,j}^{k,l}}{\partial \mathbf{q}_i} = \begin{bmatrix} \frac{\partial r_{i,j}^{k,l}}{\partial q_{i,0}} \\ \frac{\partial r_{i,j}^{k,l}}{\partial q_{i,1}} \\ \frac{\partial r_{i,j}^{k,l}}{\partial q_{i,2}} \\ \frac{\partial r_{i,j}^{k,l}}{\partial q_{i,3}} \end{bmatrix}.$$

$$\frac{\partial r_{i,j}^{k,l}}{\partial q_{i,s}} = \frac{1}{r_{i,j}^{k,l}} \left\{ (\mathbf{r}_i + R(\mathbf{q}_i)^T \mathbf{r}_i^k) - (\mathbf{r}_j + R(\mathbf{q}_j)^T \mathbf{r}_j^l) \right\} \cdot \frac{\partial R(\mathbf{q}_i)^T}{\partial q_{i,s}} \mathbf{r}_i^k, \quad [s = 0, 1, 2, 3].$$

$$\frac{\partial R(\mathbf{q}_i)^T}{\partial q_{i,0}} = \begin{bmatrix} q_{i,0} & q_{i,3} & -q_{i,2} \\ -q_{i,3} & q_{i,0} & q_{i,1} \\ q_{i,2} & -q_{i,1} & q_{i,0} \end{bmatrix}, \quad \frac{\partial R(\mathbf{q}_i)^T}{\partial q_{i,1}} = \begin{bmatrix} q_{i,1} & q_{i,2} & q_{i,3} \\ q_{i,2} & -q_{i,1} & q_{i,0} \\ q_{i,3} & -q_{i,0} & -q_{i,1} \end{bmatrix},$$

$$\frac{\partial R(\mathbf{q}_i)^T}{\partial q_{i,0}} = \begin{bmatrix} -q_{i,2} & q_{i,1} & -q_{i,0} \\ q_{i,1} & q_{i,2} & q_{i,3} \\ q_{i,0} & q_{i,3} & -q_{i,2} \end{bmatrix}, \quad \frac{\partial R(\mathbf{q}_i)^T}{\partial q_{i,1}} = \begin{bmatrix} -q_{i,3} & q_{i,0} & q_{i,1} \\ -q_{i,0} & -q_{i,3} & q_{i,2} \\ q_{i,1} & q_{i,2} & q_{i,3} \end{bmatrix}.$$

3.3.7 Boundary condition

We consider 3 possible set of boundary conditions, $c_1 - c_1$, $c_1 - c_2$ and $c_1 - c_3$, which have been described below.

1. $c_1 - c_1$: In this case, both ends are clamped. Hence, coordinates of 0^{th} and $(N+1)^{th}$ body remain same for all time.

$$\begin{aligned} \mathbf{r}_0(t) &= \mathbf{r}_0(0), & \mathbf{q}_0(t) &= \mathbf{q}_{10}(0), \\ \mathbf{r}_{N+1}(t) &= \mathbf{r}_{N+1}(0), & \mathbf{q}_{N+1}(t) &= \mathbf{q}_{N+1}(0), \\ \mathbf{p}_0(t) &= 0_{3 \times 1}, & \mathbf{g}_0(t) &= 0_{4 \times 1}, \\ \mathbf{p}_{N+1}(t) &= 0_{3 \times 1}, & \mathbf{g}_{N+1}(t) &= 0_{4 \times 1}. \end{aligned}$$

Equations (3.28a)-(3.28d) are solved for $j = 1, 2, 3, \dots, N$.

2. $c_1 - c_2$: In this case, one end is clamped and force is applied at other end, but this end is free to rotate. So, for 0^{th} body,

$$\begin{aligned}\mathbf{r}_0(t) &= \mathbf{r}_0(0), & \mathbf{q}_0(t) &= \mathbf{q}_0(0), \\ \mathbf{p}_0(t) &= 0_{3 \times 1}, & \mathbf{g}_0(t) &= 0_{4 \times 1},\end{aligned}$$

Let the applied constant force be \mathbf{F} . Then work done on the system is,

$$\mathcal{W}_F = -\mathbf{F} \cdot \mathbf{r}_{N+1}. \quad (3.31)$$

We add this work \mathcal{W}_F to the Hamiltonian of the system (3.26) and using Hamilton's equations (3.28a)-(3.28d), we get equations for $(N + 1)^{th}$ body as,

$$\begin{aligned}\frac{d\mathbf{p}_{N+1}}{dt} &= -\frac{\partial(V_{N,N+1}(\mathbf{q}_N, \mathbf{q}_{N+1}, \mathbf{r}_N, \mathbf{r}_{N+1}))}{\partial \mathbf{r}_{N+1}} + \mathbf{F}, \\ \frac{d\mathbf{r}_{N+1}}{dt} &= \frac{\mathbf{p}_{N+1}}{m_{N+1}}, \\ \frac{dg_{N+1}}{dt} &= -\frac{\partial(V_{N,N+1}(\mathbf{q}_N, \mathbf{q}_{N+1}, \mathbf{r}_N, \mathbf{r}_{N+1}))}{\partial \mathbf{q}_{N+1}} - 2\mathbf{q}_{N+1}\lambda_{N+1}, \\ \frac{d\mathbf{q}_{N+1}}{dt} &= \mu^{-1}(\mathbf{q}_{N+1})\mathbf{g}_{N+1}.\end{aligned}$$

Equations for $j = 1, 2, \dots, N$ remain same as in (3.28a)-(3.28d).

3. $c_1 - c_3$: In this case, one end is clamped and displacement \mathbf{d} is specified at other end, but this end is free to rotate. So, the boundary conditions are

$$\begin{aligned}\mathbf{r}_0(t) &= \mathbf{r}_0(0), & \mathbf{q}_0(t) &= \mathbf{q}_0(0), \\ \mathbf{p}_0(t) &= 0_{3 \times 1}, & \mathbf{g}_0(t) &= 0_{4 \times 1}, \\ \mathbf{r}_{N+1}(t) &= \mathbf{d}, & \mathbf{p}_{N+1}(t) &= 0_{3 \times 1}.\end{aligned}$$

Equations for $(N + 1)^{th}$ body are

$$\begin{aligned}\frac{d\mathbf{p}_{N+1}}{dt} &= \mathbf{0}_{3 \times 1}, \\ \frac{d\mathbf{r}_{N+1}}{dt} &= \mathbf{0}_{3 \times 1}, \\ \frac{d\mathbf{g}_{N+1}}{dt} &= -\frac{\partial(V_{N,N+1}(\mathbf{q}_N, \mathbf{q}_{N+1}, \mathbf{r}_N, \mathbf{d}))}{\partial \mathbf{q}_{N+1}} - 2\mathbf{q}_{N+1}\lambda_{N+1}, \\ \frac{d\mathbf{q}_{N+1}}{dt} &= \mu^{-1}(\mathbf{q}_{N+1})\mathbf{g}_{N+1}.\end{aligned}$$

Equations for $j = 1, 2, \dots, N$ remain same as in (3.28a)-(3.28d).

We derive the expression for the Lagrange multiplier using these Hamiltonian equations and the constraint expression. We feed this Lagrange multiplier in Hamilton's equations and solve the ODEs.

3.3.8 Expression for Lagrange multiplier λ_j

Using (3.19) and (3.28d),

$$\begin{aligned}\mathbf{q}_j^T \dot{\mathbf{q}}_j &= \frac{1}{4} \mathbf{q}_j^T \hat{G}(\mathbf{q}_j)^T [\hat{J}^{-1}] \hat{G}(\mathbf{q}_j) \mathbf{g}_j \\ &= \frac{1}{4} [1, 0, 0, 0]^T \hat{G}(\mathbf{q}_j) \mathbf{g}_j \\ &= \frac{1}{4} \mathbf{q}_j^T \mathbf{g}_j.\end{aligned}$$

Differentiating the unit quaternion constraint with respect to time, we get $\mathbf{q}_j^T \dot{\mathbf{q}}_j = 0$. Therefore,

$$\mathbf{q}_j^T \mathbf{g}_j = 0.$$

Differentiating above constraint with respect to time, we have $\mathbf{q}_j^T \dot{\mathbf{g}}_j + \dot{\mathbf{q}}_j^T \mathbf{g}_j = 0$. Using (3.28d) and (3.28d),

$$\begin{aligned}
\mathbf{q}_j^T \dot{\mathbf{g}}_j + \dot{\mathbf{q}}_j^T \mathbf{g}_j &= -\mathbf{q}_j^T \mu^{-1}(\mathbf{g}_j) \mathbf{q}_j - \mathbf{q}_j^T \frac{\partial \tilde{V}_j}{\partial \mathbf{q}_j} - 2\lambda_j \mathbf{q}_j^T \mathbf{q}_j \\
&\quad + \mathbf{g}_j^T \mu^{-1}(\mathbf{q}_j) \mathbf{g}_j. \\
\implies \lambda_j &= -\frac{1}{2} \mathbf{q}_j^T \frac{\partial \tilde{V}_j}{\partial \mathbf{q}_j},
\end{aligned} \tag{3.32}$$

where,

$$\tilde{V}_j = \begin{cases} V_{j,j+1}(\mathbf{q}_j, \mathbf{q}_{j+1}, \mathbf{r}_j, \mathbf{r}_{j+1}), & \text{if } j = 0, \\ V_{j-1,j}(\mathbf{q}_{j-1}, \mathbf{q}_j, \mathbf{r}_{j-1}, \mathbf{r}_j) \\ + V_{j,j+1}(\mathbf{q}_j, \mathbf{q}_{j+1}, \mathbf{r}_j, \mathbf{r}_{j+1}), & \text{if } 0 < j < n + 1, \\ V_{j-1,j}(\mathbf{q}_{j-1}, \mathbf{q}_j, \mathbf{r}_{j-1}, \mathbf{r}_j), & \text{if } j = N + 1. \end{cases} \tag{3.33}$$

3.3.9 Non-Dimensionalisation

We reduce number of parameters by non-dimensionalising equations by following parameters,

$$\begin{aligned}
\mathbf{r}_j &= L\tilde{\mathbf{r}}_j, \\
\mathbf{r}_j^k &= L\tilde{\mathbf{r}}_j^k, \\
m_j &= M\tilde{m}_j, \\
t &= \tau\tilde{t}.
\end{aligned}$$

Hence,

$$\begin{aligned}
\mathbf{p}_j &= m_j \frac{d\mathbf{r}_j}{dt} = \frac{ML}{\tau} \tilde{m}_j \frac{d\tilde{\mathbf{r}}_j}{d\tilde{t}} = \frac{ML}{\tau} \tilde{\mathbf{p}}_j, \\
\hat{J}^j &= ML^2 \hat{\tilde{J}}^j, \\
\mathbf{g}_j &= 4\hat{G}(\mathbf{q}_j)[\hat{\tilde{J}}]^j \hat{G}(\mathbf{q}_j)^T \dot{\mathbf{q}}_j = \frac{ML^2}{\tau} \tilde{\mathbf{g}}_j.
\end{aligned}$$

So, rewriting equations (3.28a)- (3.28d) in terms of non-dimensional entities,

$$\begin{aligned} \frac{ML^2}{\tau^2} \frac{d\tilde{\mathbf{p}}_j}{d\tilde{t}} &= -\frac{\partial(V(\mathbf{q}_{j-1}, \mathbf{q}_j, \tau\tilde{\mathbf{r}}_{j-1}, \tau\tilde{\mathbf{r}}_j) + V(\mathbf{q}_j, \mathbf{q}_{j+1}, \tau\tilde{\mathbf{r}}_j, \tau\tilde{\mathbf{r}}_{j+1}))}{\partial\tilde{\mathbf{r}}^j}, \\ \frac{d\tilde{\mathbf{r}}_j}{d\tilde{t}} &= \frac{\tilde{\mathbf{p}}_j}{\tilde{m}_j}, \\ \frac{ML^2}{\tau^2} \frac{d\tilde{\mathbf{g}}_j}{d\tilde{t}} &= -\frac{1}{4} \left(\frac{ML^2}{\tau^2} \right) \hat{G}(\tilde{\mathbf{g}}_j)^T [\hat{\tilde{J}}]^j \hat{G}(\tilde{\mathbf{g}}_j) \mathbf{q}_j \\ &\quad - \frac{\partial(V(\mathbf{q}_{j-1}, \mathbf{q}_j, \tau\tilde{\mathbf{r}}_{j-1}, \tau\tilde{\mathbf{r}}_j) + V(\mathbf{q}_j, \mathbf{q}_{j+1}, \tau\tilde{\mathbf{r}}_j, \tau\tilde{\mathbf{r}}_{j+1}))}{\partial\mathbf{q}_j} \\ &\quad - 2\lambda_j \mathbf{q}_j, \\ \frac{d\mathbf{q}_j}{d\tilde{t}} &= \frac{1}{4} \hat{G}(\mathbf{q}_j)^T [\hat{\tilde{J}}]^j \hat{G}(\mathbf{q}_j) \tilde{\mathbf{g}}_j. \end{aligned}$$

We have derived Hamilton's equations for three dimensional chain in terms of quaternion. The main challenge in the formalism is forcing the unit quaternion constraint. We have derived the expression for Lagrange multiplier for continuous ODEs.

After introducing this multiplier, we estimate the order of error in unit quaternion constraint. We derive the order of error analytically for *Euler-B* scheme and numerically for higher order algorithms. Also, we prove the symplecticity of the algorithm for Euler-A symplectic scheme. We are using *Gauss6* symplectic sixth order scheme to solve the chain problem, but providing analytical proof for order of unit quaternion constraint and symplecticity of this algorithm is bit difficult. However, this can be done in similar way as we demonstrate it for *Euler-B* and *Euler-A* scheme.

3.4 Order and Symplecticity of constrained algorithm

Let the conjugate pairs of the Hamiltonian system be $(\mathbf{p}_j, \mathbf{r}_j)_{j=0,1,\dots,N+1}$ and $(\mathbf{g}_j, \mathbf{q}_j)_{j=0,1,\dots,N+1}$.

Hamiltonian of the constrained system is,

$$\begin{aligned} \mathcal{H}(\mathbf{p}_0, \mathbf{p}_1, \dots, \mathbf{p}_{N+1}, \mathbf{r}_0, \mathbf{r}_1, \dots, \mathbf{r}_{N+1}, \mathbf{g}_0, \mathbf{g}_1, \dots, \mathbf{g}_{N+1}, \mathbf{q}_0, \mathbf{q}_1, \dots, \mathbf{q}_{N+1}) \\ = \tilde{\mathcal{H}}(\mathbf{p}_0, \mathbf{p}_1, \dots, \mathbf{p}_{N+1}, \mathbf{r}_0, \mathbf{r}_1, \dots, \mathbf{r}_{N+1}, \mathbf{g}_0, \mathbf{g}_1, \dots, \mathbf{g}_{N+1}, \mathbf{q}_0, \mathbf{q}_1, \dots, \mathbf{q}_{N+1}) + \sum_{j=0}^{N+1} \lambda_j (\mathbf{q}_j^T \mathbf{q}_j - 1). \end{aligned} \tag{3.34}$$

where,

$$\tilde{\mathcal{H}} = \sum_{j=0}^{N+1} \frac{1}{2} \mathbf{g}_j^T \mu^{-1}(\mathbf{q}_j) \mathbf{g}_j + \sum_{j=0}^{N+1} \frac{\mathbf{p}_j^2}{2m_j} + \sum_{j=0}^N V_{j,j+1}(\mathbf{q}_j, \mathbf{q}_{j+1}, \mathbf{r}_j, \mathbf{r}_{j+1}). \quad (3.35)$$

Let the step size of the discretization be h . Let $(\cdot)_j^k$ denote (\cdot) value of j^{th} body at k^{th} step. When we solve for $(\mathbf{p}_j, \mathbf{r}_j)$ and $(\mathbf{g}_j, \mathbf{q}_j)$, Hamiltonian is the function of these variables only.

3.4.1 Order of the constrained algorithm

Using *Euler-B*, a symplectic scheme, we show here, the order of error in the constraints $\mathbf{q}_j^T \mathbf{q}_j = 1$ and $\mathbf{q}_j^T \mathbf{g}_j = 0$. *Euler-B* discretization for conjugate pair $(\mathbf{g}_j, \mathbf{q}_j)$ is:

$$\mathbf{q}_j^{n+1} = \mathbf{q}_j^n + h \tilde{\mathcal{H}}_g(\mathbf{g}_j^{n+1}, \mathbf{q}_j^n), \quad (3.36)$$

$$\mathbf{g}_j^{n+1} = \mathbf{g}_j^n - h \tilde{\mathcal{H}}_q(\mathbf{g}_j^{n+1}, \mathbf{q}_j^n) - 2\lambda_j h \mathbf{q}_j^n. \quad (3.37)$$

Using (3.28d), (3.28d) and (3.33)

$$\begin{aligned} \tilde{\mathcal{H}}_g(\mathbf{g}_j^{n+1}, \mathbf{q}_j^n) &= \mu^{-1}(\mathbf{q}_j^n) \mathbf{g}_j^{n+1}, \\ \tilde{\mathcal{H}}_q(\mathbf{g}_j^{n+1}, \mathbf{q}_j^n) &= \mu^{-1}(\mathbf{g}_j^{n+1}) \mathbf{q}_j^n + \frac{\partial \tilde{V}}{\partial \mathbf{q}_j}, \\ \lambda_j &= -\frac{1}{2} \mathbf{q}_j^{nT} \frac{\partial \tilde{V}}{\partial \mathbf{q}_j}. \end{aligned}$$

where, $\frac{\partial \tilde{V}}{\partial \mathbf{q}_j}$ is valuated at $(\mathbf{g}_j^{n+1}, \mathbf{q}_j^n)$.

Unit quaternion constraint

$$\begin{aligned} (\mathbf{q}_j^{n+1})^T \mathbf{q}_j^{n+1} &= \{ \mathbf{q}_j^{nT} + h(\mathbf{g}_j^{n+1})^T \mu^{-1}(\mathbf{q}_j^n) \} \{ \mathbf{q}_j^n + h \mu^{-1}(\mathbf{q}_j^n) \mathbf{g}_j^{n+1} \} \\ &= \mathbf{q}_j^{nT} \mathbf{q}_j^N + 2h \mathbf{q}_j^{nT} \mu^{-1}(\mathbf{q}_j^n) \mathbf{g}_j^{n+1} + h^2 (\mathbf{g}_j^{n+1})^T \mu^{-1}(\mathbf{q}_j^n) \mu^{-1}(\mathbf{q}_j^n) \mathbf{g}_j^{n+1}. \end{aligned}$$

Using 3.18, we see that

$$\begin{aligned}
\mathbf{q}_j^{nT} \mu^{-1}(\mathbf{q}_j^n) \mathbf{g}_j^{n+1} &= 4\mathbf{q}_j^{nT} \hat{G}(\mathbf{q}_j^n)^T [\hat{J}]^j \hat{G}(\mathbf{q}_j^n) \mathbf{g}_j^{n+1} \\
&= 4\mathbf{q}_j^{nT} \hat{G}(\mathbf{q}_j)^T [\hat{J}^{-1}] \hat{G}(\mathbf{q}_j^n) \mathbf{g}_j^{n+1} \\
&= 4[1, 0, 0, 0] \hat{G}(\mathbf{q}_j^n) \mathbf{g}_j^{n+1} \\
&= 4\mathbf{q}_j^{nT} \mathbf{g}_j^{n+1} \\
&= 4\mathbf{q}_j^{nT} \mathbf{g}_j^n + O(h). \quad [\text{Using 3.37}]
\end{aligned}$$

Assuming that $\mathbf{q}_j^{nT} \mathbf{q}_j^n = 1$ and $\mathbf{q}_j^{nT} \mathbf{g}_j^n = 0$, we have,

$$(\mathbf{q}_j^{n+1})^T \mathbf{q}_j^{n+1} = 1 + O(h^2). \quad (3.38)$$

Constraint on conjugate momenta

$$\begin{aligned}
(\mathbf{q}_j^{n+1})^T \mathbf{g}_j^{n+1} &= \{\mathbf{q}_j^{nT} + h(\mathbf{g}_j^{n+1})^T \mu^{-1}(\mathbf{q}_j^n)\} \{\mathbf{g}_j^n - h\mu^{-1}(\mathbf{g}_j^{n+1})\mathbf{q}_j^n \\
&\quad - h \frac{\partial \tilde{V}}{\partial \mathbf{q}_j} + h \left(\mathbf{q}_j^{nT} \frac{\partial \tilde{V}}{\partial \mathbf{q}_j} \right) \mathbf{q}_j^n\} \\
&= \mathbf{q}_j^{nT} \mathbf{g}_j^n - h\{(\mathbf{g}_j^{n+1})^T \mu^{-1}(\mathbf{q}_j^n) \mathbf{g}_j^n + \mathbf{q}_j^{nT} \mu^{-1}(\mathbf{g}_j^{n+1}) \mathbf{q}_j^n\} \\
&\quad - h\mathbf{q}_j^{nT} \frac{\partial \tilde{V}}{\partial \mathbf{q}_j} + h\mathbf{q}_j^{nT} \mathbf{q}_j^N \left(\mathbf{q}_j^{nT} \frac{\partial \tilde{V}}{\partial \mathbf{q}_j} \right) + O(h^2).
\end{aligned}$$

Using (3.37) and the property

$$\mathbf{g}_j^T \mu^{-1}(\mathbf{q}_j) \mathbf{g}_j = \mathbf{q}_j^T \mu^{-1}(\mathbf{g}_j) \mathbf{q}_j,$$

we have,

$$\begin{aligned}
(\mathbf{g}_j^{n+1})^T \mu^{-1}(\mathbf{q}_j^n) \mathbf{g}_j^n &= (\mathbf{g}_j^{n+1})^T \mu^{-1}(\mathbf{q}_j^n) \mathbf{g}_j^{n+1} + O(h) \\
&= \mathbf{q}_j^{nT} \mu^{-1}(\mathbf{g}_j^{n+1}) \mathbf{g}_j^{n+1} + O(h).
\end{aligned}$$

Using above expression and assuming that $\mathbf{q}_j^{nT} \mathbf{q}_j^n = 1$ and $\mathbf{q}_j^{nT} \mathbf{g}_j^n = 0$,

$$(\mathbf{q}_j^{n+1})^T \mathbf{g}_j^{n+1} = 0 + O(h^2). \quad (3.39)$$

We conclude from equations (3.38) and (3.39) that *Euler-B* scheme respect the constraints ($\mathbf{q}_j^T \mathbf{q}_j = 1$) and ($\mathbf{q}_j^T \mathbf{g}_j = 0$) upto second order.

For a typical symmetric top problem, we plot the error in quaternion constraint vs step size for the higher order symplectic algorithms. In the figure 3.3, we see that all the symplectic

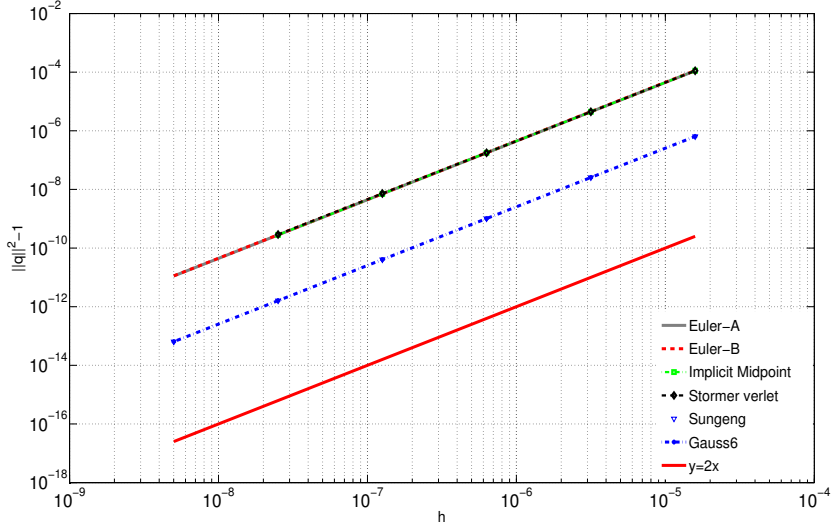


FIGURE 3.3: Error in unit quaternion vs step size for symplectic algorithms

algorithms, second order schemes *Implicit-midpoint* and *Stormer-Verlet*, fifth order scheme *Sungeng* and sixth order scheme *Gauss6* respect the unit quaternion constraint upto second order only. However, *Gauss6*, being a higher order algorithm, has least magnitude of error compared to rest of the algorithms.

3.4.2 Symplecticity of the constrained algorithm

We use first order symplectic *Euler-A* scheme. *Euler-A* discretization is given by

$$\begin{aligned}\mathbf{r}_j^{n+1} &= \mathbf{r}_j^n + h\tilde{\mathcal{H}}_{\mathbf{p}}(\mathbf{p}_j^n, \mathbf{r}_j^{n+1}), \\ \mathbf{p}_j^{n+1} &= \mathbf{p}_j^n - h\tilde{\mathcal{H}}_{\mathbf{r}}(\mathbf{p}_j^n, \mathbf{r}_j^{n+1}), \\ \mathbf{q}_j^{n+1} &= \mathbf{q}_j^n + h\tilde{\mathcal{H}}_{\mathbf{g}}(\mathbf{g}_j^n, \mathbf{q}_j^{n+1}), \\ \mathbf{g}_j^{n+1} &= \mathbf{g}_j^n - h\tilde{\mathcal{H}}_{\mathbf{q}}(\mathbf{g}_j^n, \mathbf{q}_j^{n+1}) - 2\lambda_j \mathbf{q}_j^{n+1}.\end{aligned}$$

Taking *one-form* of the above discretization,

$$d\mathbf{r}_j^{n+1} = d\mathbf{r}_j^n + hd\tilde{\mathcal{H}}_{\mathbf{p}}(\mathbf{p}_j^n, \mathbf{r}_j^{n+1}), \quad (3.40a)$$

$$d\mathbf{p}_j^{n+1} = d\mathbf{p}_j^n - hd\tilde{\mathcal{H}}_{\mathbf{r}}(\mathbf{p}_j^n, \mathbf{r}_j^{n+1}), \quad (3.40b)$$

$$d\mathbf{q}_j^{n+1} = d\mathbf{q}_j^n + hd\tilde{\mathcal{H}}_{\mathbf{g}}(\mathbf{g}_j^n, \mathbf{q}_j^{n+1}), \quad (3.40c)$$

$$d\mathbf{g}_j^{n+1} = d\mathbf{g}_j^n - hd\tilde{\mathcal{H}}_{\mathbf{q}}(\mathbf{g}_j^n, \mathbf{q}_j^{n+1}) - 2\lambda_j \mathbf{q}_j^{n+1}. \quad (3.40d)$$

Using chain rule,

$$d\tilde{\mathcal{H}}_{\mathbf{p}}(\mathbf{p}_j^n, \mathbf{r}_j^{n+1}) = \tilde{\mathcal{H}}_{\mathbf{pp}} d\mathbf{p}_j^n + \tilde{\mathcal{H}}_{\mathbf{pr}} \overset{0}{\cancel{d\mathbf{r}_j^{n+1}}}, \quad (3.41a)$$

$$d\tilde{\mathcal{H}}_{\mathbf{r}}(\mathbf{p}_j^n, \mathbf{r}_j^{n+1}) = \tilde{\mathcal{H}}_{\mathbf{rp}} \overset{0}{\cancel{d\mathbf{p}_N}} + \tilde{\mathcal{H}}_{\mathbf{rr}} d\mathbf{r}_j^{n+1}, \quad (3.41b)$$

$$d\tilde{\mathcal{H}}_{\mathbf{g}}(\mathbf{g}_j^n, \mathbf{q}_j^{n+1}) = \tilde{\mathcal{H}}_{\mathbf{gg}} d\mathbf{g}_j^n + \tilde{\mathcal{H}}_{\mathbf{gq}} d\mathbf{q}_j^{n+1}, \quad (3.41c)$$

$$d\tilde{\mathcal{H}}_{\mathbf{q}}(\mathbf{g}_j^n, \mathbf{q}_j^{n+1}) = \tilde{\mathcal{H}}_{\mathbf{qg}} d\mathbf{g}_j^n + \tilde{\mathcal{H}}_{\mathbf{qq}} d\mathbf{q}_j^{n+1} - 2\lambda_j d\mathbf{q}_j^{n+1} - 2\mathbf{q}_j^{n+1} d\lambda_j. \quad (3.41d)$$

Some properties of wedge products are,

$$d\mathbf{a} \wedge d\mathbf{a} = 0, \quad d\mathbf{a} \wedge d\mathbf{b} = -d\mathbf{b} \wedge d\mathbf{a}, \quad d\mathbf{a} \wedge (A\mathbf{a}) = (A^T d\mathbf{a}) \wedge d\mathbf{a} \quad (3.42)$$

From (3.40a) and (3.40b) and using (3.41a) and (3.41b),

$$d\mathbf{r}_j^{n+1} \wedge d\mathbf{p}_j^n = d\mathbf{r}_j^n \wedge d\mathbf{p}_j^n + h\tilde{\mathcal{H}}_{\mathbf{pp}} d\mathbf{p}_j^n \wedge \overset{0}{\cancel{d\mathbf{p}_j^{n+1}}}, \quad (3.43a)$$

$$d\mathbf{r}_j^{n+1} \wedge d\mathbf{p}_j^{n+1} = d\mathbf{r}_j^{n+1} \wedge d\mathbf{p}_j^n - h\tilde{\mathcal{H}}_{\mathbf{rr}} \overset{0}{\cancel{d\mathbf{r}_j^{n+1}}} \wedge \overset{0}{\cancel{d\mathbf{r}_j^{n+1}}}. \quad (3.43b)$$

Adding above two equations,

$$d\mathbf{r}_j^{n+1} \wedge d\mathbf{p}_j^{n+1} = d\mathbf{r}_j^n \wedge d\mathbf{p}_j^n. \quad (3.44)$$

From (3.40c) and (3.40d) and using (3.41c) and (3.41d),

$$\begin{aligned} d\mathbf{q}_j^{n+1} \wedge d\mathbf{g}_j^n &= d\mathbf{q}_j^n \wedge d\mathbf{g}_j^n + h\tilde{\mathcal{H}}_{\mathbf{gg}} d\mathbf{g}_j^n \wedge \overset{0}{\cancel{d\mathbf{g}_j^{n+1}}} + h\tilde{\mathcal{H}}_{\mathbf{gq}} d\mathbf{q}_j^{n+1} \wedge d\mathbf{g}_j^n, \\ d\mathbf{q}_j^{n+1} \wedge d\mathbf{g}_j^{n+1} &= d\mathbf{q}_j^{n+1} \wedge d\mathbf{g}_j^n - h\tilde{\mathcal{H}}_{\mathbf{qg}}^T d\mathbf{g}_j^n, d\mathbf{q}_j^{n+1} \wedge d\mathbf{g}_j^n - h\tilde{\mathcal{H}}_{\mathbf{qq}} d\mathbf{q}_j^{n+1} \wedge \overset{0}{\cancel{d\mathbf{q}_j^{n+1}}} \\ &\quad - 2\lambda_j d\mathbf{q}_j^{n+1} \wedge \overset{0}{\cancel{d\mathbf{q}_j^{n+1}}} - 2(\mathbf{q}_j^{n+1})^T d\mathbf{q}_j^{n+1} \wedge d\lambda_j. \end{aligned}$$

Adding above two equations,

$$d\mathbf{q}_j^{n+1} \wedge d\mathbf{g}_j^{n+1} = d\mathbf{q}_j^n \wedge d\mathbf{g}_j^n - 2(\mathbf{q}_j^{n+1})^T d\mathbf{q}_j^{n+1} \wedge d\lambda_j.$$

From the equation 3.38,

$$\begin{aligned} (\mathbf{q}_j^{n+1})^T \mathbf{q}_j^{n+1} &= 1 + O(h^2), \\ \implies (\mathbf{q}_j^{n+1})^T d\mathbf{q}_j^{n+1} &= 0. \end{aligned}$$

Hence,

$$(\mathbf{q}_j^{n+1})^T d\mathbf{q}_j^{n+1} \wedge d\lambda_j = 0, \quad \forall \lambda_j.$$

Therefore,

$$d\mathbf{q}_j^{n+1} \wedge d\mathbf{g}_j^{n+1} = d\mathbf{q}_j^n \wedge d\mathbf{g}_j^n. \quad (3.45)$$

We conclude from above subsection that addition of Lagrange multiplier successfully force the unit quaternion constraint upto second order. We also see that addition of the constraint term to the Hamiltonian of the system does not destroy its symplecticity. We, now have the Hamiltonian formulation for the three dimensional chain of rigid bodies in terms of quaternion.

3.5 Example

The figure above shows a tetrahedron with particles at its vertices attached through rigid link. Let us assume mass of each particle to be m . Let us denote position vector of k^{th} particle of i^{th} body in body fixed frame as \mathbf{r}_i^k .

$$\begin{aligned} \mathbf{r}_i^1 &= -\frac{a}{2}\mathbf{e}_1^i - \frac{a}{3}\mathbf{e}_2^i - \frac{a}{4}\mathbf{e}_3^i, \\ \mathbf{r}_i^2 &= \frac{a}{2}\mathbf{e}_1^i - \frac{a}{3}\mathbf{e}_2^i - \frac{a}{4}\mathbf{e}_3^i, \\ \mathbf{r}_i^1 &= 0\mathbf{e}_1^i + \frac{2a}{3}\mathbf{e}_2^i - \frac{a}{4}\mathbf{e}_3^i, \\ \mathbf{r}_i^1 &= 0\mathbf{e}_1^i + 0\mathbf{e}_2^i + \frac{3a}{4}\mathbf{e}_3^i. \end{aligned}$$

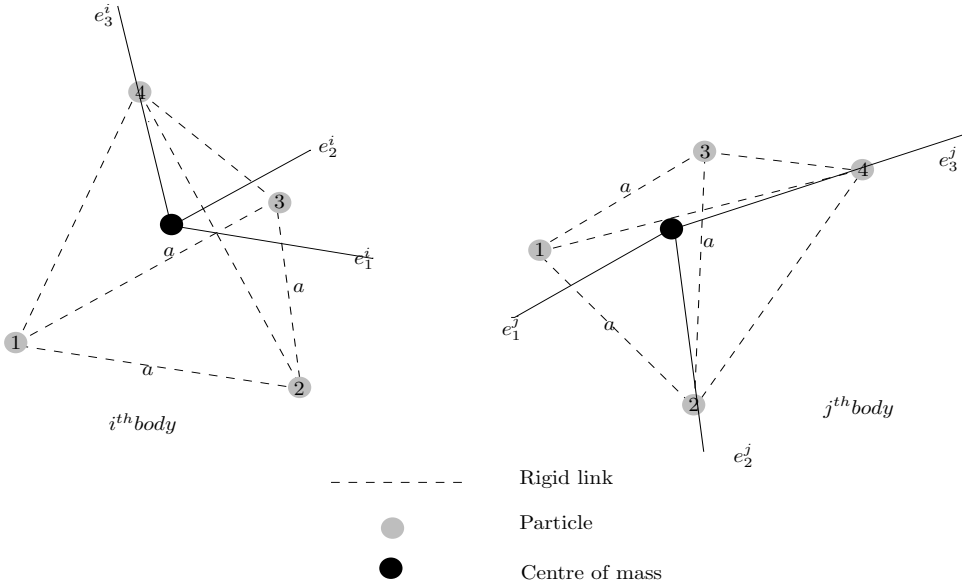


FIGURE 3.4: Rigid tetrahedron

Moment of inertia of the tetrahedron is given as

$$\begin{aligned}
 I_{11} &= \sum_{k=1}^4 m_k(y_k^2 + z_k^2) = \frac{17a^2}{12}, \\
 I_{22} &= \sum_{k=1}^4 m_k(x_k^2 + z_k^2) = \frac{5a^2}{4}, \\
 I_{33} &= \sum_{k=1}^4 m_k(x_k^2 + y_k^2) = \frac{5a^2}{6}, \\
 I_{12} &= I_{13} = I_{23} = 0.
 \end{aligned}$$

3.5.1 Potential energy

We assume Lennard-Jones potential [24] interaction between two tetrahedrons. So the potential energy contribution from two particles, k, l of i^{th} and j^{th} body respectively is given by

$$V_{ij}^{k,l} = 4\epsilon \left[\left(\frac{\sigma}{r_{i,j}^{k,l}} \right)^{12} - \left(\frac{\sigma}{r_{i,j}^{k,l}} \right)^6 \right],$$

where, $r_{i,j}^{k,l}$ (from (3.29)) denotes distance between k particle of i^{th} body and l particle of j^{th} body.

So, potential energy contribution from pair i^{th} and j^{th} body is,

$$V_{ij} = \sum_{k=1}^4 \sum_{l=1}^4 V_{ij}^{k,l}.$$

Partial differentiation of V^{ij} with respect to \mathbf{r}^i and \mathbf{q}_i^i are,

$$\begin{aligned}\frac{\partial V_{ij}}{\partial \mathbf{r}_i} &= \sum_{k=1}^4 \sum_{l=1}^4 \frac{\partial V_{ij}^{k,l}}{\partial \mathbf{r}_i}, \\ \frac{\partial V_{ij}}{\partial \mathbf{q}_i} &= \sum_{k=1}^4 \sum_{l=1}^4 \frac{\partial V_{ij}^{k,l}}{\partial \mathbf{q}_i}.\end{aligned}$$

$$\begin{aligned}\frac{\partial V_{ij}^{k,l}}{\partial \mathbf{r}_i} &= -\frac{24\epsilon}{\sigma} \left[2 \left(\frac{\sigma}{r_{i,j}^{k,l}} \right)^{13} - \left(\frac{\sigma}{r_{i,j}^{k,l}} \right)^7 \right] \frac{\partial r_{i,j}^{k,l}}{\partial \mathbf{r}_i}, \\ \frac{\partial V_{ij}^{k,l}}{\partial \mathbf{q}_i} &= -\frac{24\epsilon}{\sigma} \left[2 \left(\frac{\sigma}{r_{i,j}^{k,l}} \right)^{13} - \left(\frac{\sigma}{r_{i,j}^{k,l}} \right)^7 \right] \frac{\partial r_{i,j}^{k,l}}{\partial \mathbf{q}_i},\end{aligned}$$

where, $\frac{\partial r_{i,j}^{k,l}}{\partial \mathbf{r}_i}$ and $\frac{\partial r_{i,j}^{k,l}}{\partial \mathbf{q}_i}$ are obtained from (3.3.6) and (3.3.6) respectively.

We, solve the above example for the system containing 8 tetrahedrons, using sixth order symplectic *Gauss6* scheme for a typical initial velocity, and following parameters.

$$a = 1\text{m}, \text{mass} = 1\text{kg}, \mathbf{r}_i(0) = (2i, 0, 0), i = 1, 2, \dots, 8, \mathbf{F} = (3, 0, 0), \epsilon = 5, \sigma = 1.$$

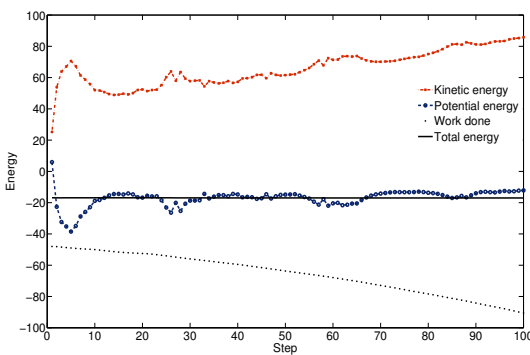


FIGURE 3.5: Energy(in J) vs number of steps for c1-c2 boundary condition

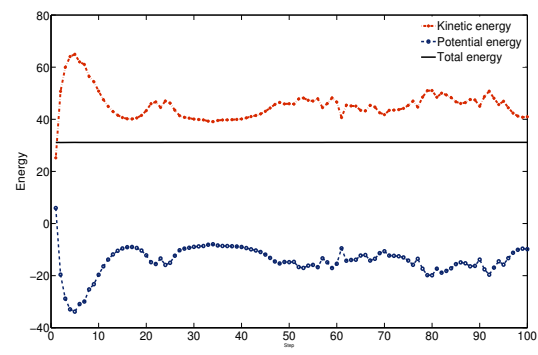


FIGURE 3.6: Energy(in J) vs number of steps for c1-c1 boundary condition

Figure 3.5 and 3.6 show the energy of the system for c1-c2 (clamped-constant force) and c1-c1 (clamped-clamped) boundary condition respectively. Hamiltonian of the system remain conserved in both the cases. Hence our formulation of the chain problem successfully conserve the Hamiltonian of the system.

Computation time We observe the effect of number of bodies and the effect of number of particle in the body on computation time. We use disc shape of rigid body as the example. Particles are assumed to be uniformly distributed on the circumference of two circles forming faces of the disc. For a typical initial condition, parameters used are,

radius of disc $a = .05m$, thickness $t = a/10$, $\sigma = 1$, $\epsilon = 10^{-6}$, $\mathbf{F} = .03N$ in x direction,

where, \mathbf{F} is the force applied at last body.

The calculation has been done using *Gauss6* scheme with step size $h = .01$ and tolerance 10^{-9} . The machine used is eight core “Intel(R) Xenon cpu ES420 @2.50GHz”

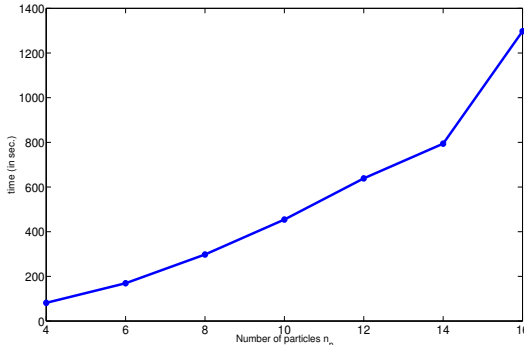


FIGURE 3.7: Number of particle n_p vs time for Number of body N = 6

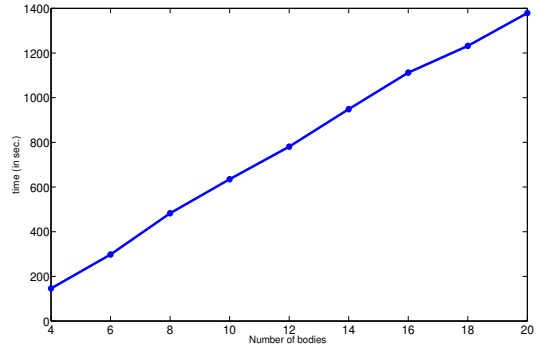


FIGURE 3.8: Number of body N vs time for number of particle=12

Figures clearly show the increase in computation time as number of bodies/ particles are increased.

In order to demonstrate the accuracy of unit quaternion constraint, we plot the error in quaternions for the system with parameters as defined above and number of bodies = 8 and number of particles = 8.

Figure 3.9 shows that quaternions remain unit to a good extent for all the bodies in the chain.

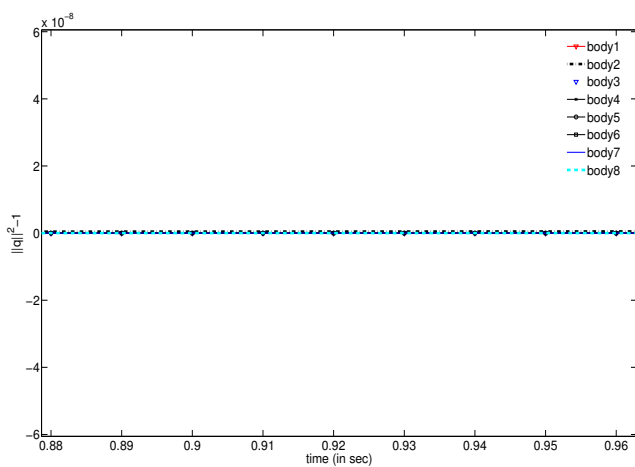


FIGURE 3.9: Error in unit quaternion for different bodies

Chapter 4

Conclusion and Future work

4.1 Conclusion

We have successfully established a Hamiltonian formulation for a chain of rigid bodies using Rotation matrix and quaternions as rotation parameters. We have modeled rigid bodies as an array of particles attached to each other through rigid links. Therefore, our formulation can be used for any shape of the rigid body.

We have introduced the Lagrangian multiplier into already existing symplectic algorithms and have achieved a second order algorithm with respect to unit quaternion constraint. We have also shown that introduction of the Lagrange multiplier into Hamiltonian system does not affect the symplecticity of the system. In the figure 3.7 and 3.8, we have shown computation time for different sets of number of particles and number of bodies. Figures suggest that algorithm used is significantly fast and hence can be applied for large number of bodies.

4.2 Future Work

A symplectic algorithm conserving the unit quaternion constraint upto higher order can be devised. When the equation of motion for the chain of rigid bodies is linearized about its equilibrium position, we are able to calculate the natural frequency of the system. This

natural frequency can be used has a parameter to compare the motion of a chain of large number of rigid bodies and a Cosserat rod.

Appendix A

Rotation matrix

A.1 Rotation matrix in terms of quaternions

Quaternions corresponding to j^{th} body is defined as,

$$\mathbf{q}^j = q_{j,0} + q_{j,1}\mathbf{e}_1 + q_{j,2}\mathbf{e}_2 + q_{j,3}\mathbf{e}_3 \quad (\text{A.1})$$

We derive a rotation tensor $\mathbf{R}(\mathbf{q}^j)$ which relates basis $\{e_i^j\}_{i=1,2,3}$ of j^{th} body fixed frame to stationary frame basis $\{e_i\}_{i=1,2,3}$. Quaternions represent rotation iff their mod is unity, i.e.,

$$||\mathbf{q}^j||^2 = q_{j,0}^2 + q_{j,1}^2 + q_{j,2}^2 + q_{j,3}^2 = 1 \quad (\text{A.2})$$

From here onwards, we consider unit quaternion only. The quaternion can be used to describe rotation about an axis \mathbf{r} through an angle ϕ as

$$\mathbf{q}^j = \cos \frac{\phi}{2} + \sin \frac{\phi}{2} \mathbf{r} \quad (\text{A.3})$$

i.e.,

$$q_{j,0} = \cos \frac{\phi}{2}, \quad q_{j,1} = \sin \frac{\phi}{2} r_1, \quad q_{j,2} = \sin \frac{\phi}{2} r_2, \quad q_{j,3} = \sin \frac{\phi}{2} r_3, \quad (\text{A.4})$$

where r_i is i^{th} component of unit vector \mathbf{r} .

Using Rodrigue's rotation formula, if a vector \mathbf{v} is rotated by angle ϕ about an axis \mathbf{r} , then

the rotated vector is given by,

$$\mathbf{v}^{rot} = \mathbf{v} \cos \phi + (\mathbf{r} \times \mathbf{v}) \sin \phi + \mathbf{r}(\mathbf{r} \cdot \mathbf{v})(1 - \cos \phi) \quad (\text{A.5})$$

We derive the rotation matrix corresponding to this rotation in terms of quaternion as

$$\mathbf{v}^{rot} = \mathbf{v} \cos \phi + (\mathbf{r} \times \mathbf{v}) \sin \phi + \mathbf{r}(\mathbf{r} \cdot \mathbf{v})(1 - \cos \phi) \quad (\text{A.6})$$

$$= \mathbf{v}(2 \cos^2 \frac{\phi}{2} - 1) + 2\tilde{\mathbf{r}} \sin \frac{\phi}{2} \cos \frac{\phi}{2} \mathbf{v} + 2 \sin^2 \frac{\phi}{2} (\mathbf{r} \otimes \mathbf{r}) \mathbf{v} \quad (\text{A.7})$$

$$= \mathbf{R}\mathbf{v}, \quad (\text{A.8})$$

where $\tilde{\mathbf{r}}$ is the skew tensor corresponding to axial vector \mathbf{r} and $\mathbf{R}(\mathbf{q}^j)$ is the rotation tensor given by,

$$\begin{aligned} \mathbf{R} &= (2 \cos^2 \frac{\phi}{2} - 1) \mathbf{I} + 2\tilde{\mathbf{r}} \sin \frac{\phi}{2} \cos \frac{\phi}{2} + 2 \sin^2 \frac{\phi}{2} (\mathbf{r} \otimes \mathbf{r}) \\ &= (2q_{j,0}^2 - 1) \mathbf{I} + 2 \cos \frac{\phi}{2} \begin{bmatrix} 0 & -r_3 \sin \frac{\phi}{2} & r_2 \sin \frac{\phi}{2} \\ r_3 \sin \frac{\phi}{2} & 0 & -r_1 \sin \frac{\phi}{2} \\ -r_2 \sin \frac{\phi}{2} & r_1 \sin \frac{\phi}{2} & 0 \end{bmatrix} \quad (\text{A.9}) \end{aligned}$$

$$+ 2 \begin{bmatrix} r_1^2 \sin^2 \frac{\phi}{2} & r_1 r_2 \sin^2 \frac{\phi}{2} & r_1 r_3 \sin^2 \frac{\phi}{2} \\ r_2 r_1 \sin^2 \frac{\phi}{2} & r_2^2 \sin^2 \frac{\phi}{2} & r_2 r_3 \sin^2 \frac{\phi}{2} \\ r_3 r_1 \sin^2 \frac{\phi}{2} & r_3 r_2 \sin^2 \frac{\phi}{2} & r_3^2 \sin^2 \frac{\phi}{2} \end{bmatrix} \quad (\text{A.10})$$

Components of this tensor is represented by matrix R .

$$\begin{aligned} \mathbf{R}(\mathbf{q}^j) &= (2q_{j,0}^2 - 1) \mathbf{I} + 2q_{j,0} \begin{bmatrix} 0 & -q_{j,3} & q_{j,2} \\ q_{j,3} & 0 & -q_{j,1} \\ -q_{j,2} & q_{j,1} & 0 \end{bmatrix} + 2 \begin{bmatrix} q_{j,1}^2 & q_{j,1}q_{j,2} & q_{j,1}q_{j,3} \\ q_{j,2}q_{j,1} & q_{j,2}^2 & q_{j,2}q_{j,3} \\ q_{j,3}q_{j,1} & q_{j,3}q_{j,2} & q_{j,3}^2 \end{bmatrix} \\ &= \begin{bmatrix} 2q_{j,0}^2 + 2q_{j,1}^2 - 1 & 2q_{j,1}q_{j,2} - 2q_{j,0}q_{j,3} & 2q_{j,1}q_{j,3} + 2q_{j,0}q_{j,2} \\ 2q_{j,1}q_{j,2} + 2q_{j,0}q_{j,3} & 2q_{j,0}^2 + 2q_{j,2}^2 - 1 & 2q_{j,2}q_{j,3} - 2q_{j,0}q_{j,1} \\ 2q_{j,3}q_{j,1} - 2q_{j,0}q_{j,2} & 2q_{j,3}q_{j,2} + 2q_{j,0}q_{j,1} & 2q_{j,0}^2 + 2q_{j,3}^2 - 1 \end{bmatrix} \quad (\text{A.11}) \end{aligned}$$

Angular velocity $\omega(\mathbf{q}^j, \dot{\mathbf{q}}^j)$ is the axial vector of skew symmetric tensor $\dot{\mathbf{R}}\mathbf{R}^T$. Angular velocity of j^{th} body in body fixed basis $\{e_i^j\}_{i=1,2,3}$ is,

$$\omega^j(\mathbf{q}^j, \dot{\mathbf{q}}^j) = \text{axial}(\dot{\mathbf{R}}\mathbf{R}^T) = 2G(\mathbf{q}^j) \begin{bmatrix} \dot{q}_{j,0} \\ \dot{q}_{j,1} \\ \dot{q}_{j,2} \\ \dot{q}_{j,3} \end{bmatrix} \quad (\text{A.12})$$

where,

$$G(\mathbf{q}^j) = \begin{bmatrix} -q_{j,1} & q_{j,0} & q_{j,3} & -q_{j,2} \\ -q_{j,2} & -q_{j,3} & q_{j,0} & q_{j,1} \\ -q_{j,3} & q_{j,2} & -q_{j,1} & q_{j,0} \end{bmatrix} \quad (\text{A.13})$$

A.2 Euler angle and quaternions

If a frame is rotated by angle θ about axis \mathbf{n} , then quaternion corresponding to this rotation is given by

$$\mathbf{q}_n(\theta) = \cos \theta/2 + \mathbf{n} \sin \theta/2 \quad (\text{A.14})$$

We choose **ZYZ** class of rotation. So quaternions associating body fixed frame $\{e_i\}$ with stationary frame $\{E_i\}$ is given by

$$\mathbf{q} = \mathbf{q}_z(\phi)\mathbf{q}_y(\theta)\mathbf{q}_z(\psi) \quad (\text{A.15})$$

$$\begin{aligned} \mathbf{q} &= (\cos \phi/2 + \mathbf{k} \sin \phi/2)(\cos \theta/2 + \mathbf{j} \sin \theta/2)(\cos \psi/2 + \mathbf{k} \sin \psi/2) \\ &= \cos \frac{\theta}{2} \cos \left(\frac{\phi + \psi}{2} \right) + i \sin \frac{\theta}{2} \sin \left(\frac{\phi + \psi}{2} \right) \\ &\quad + j \sin \frac{\theta}{2} \cos \left(\frac{\phi + \psi}{2} \right) + k \cos \frac{\theta}{2} \sin \left(\frac{\phi + \psi}{2} \right) \end{aligned} \quad (\text{A.16})$$

So, the component of quaternion are,

$$\begin{aligned}
q_0 &= \cos \frac{\theta}{2} \cos \left(\frac{\phi + \psi}{2} \right) \\
q_1 &= \sin \frac{\theta}{2} \sin \left(\frac{\phi + \psi}{2} \right) \\
q_2 &= \sin \frac{\theta}{2} \cos \left(\frac{\phi + \psi}{2} \right) \\
q_3 &= \cos \frac{\theta}{2} \sin \left(\frac{\phi + \psi}{2} \right)
\end{aligned} \tag{A.17}$$

Differentiating above equations with respect to time,

$$\dot{q}_0 = -\sin \frac{\theta}{2} \cos \left(\frac{\phi + \psi}{2} \right) \frac{\dot{\theta}}{2} - \cos \frac{\theta}{2} \sin \left(\frac{\phi + \psi}{2} \right) \frac{\dot{\phi} + \dot{\psi}}{2} \tag{A.18}$$

$$\dot{q}_1 = \cos \frac{\theta}{2} \sin \left(\frac{\phi + \psi}{2} \right) \frac{\dot{\theta}}{2} + \sin \frac{\theta}{2} \cos \left(\frac{\phi + \psi}{2} \right) \frac{\dot{\phi} + \dot{\psi}}{2} \tag{A.19}$$

$$\dot{q}_2 = \cos \frac{\theta}{2} \cos \left(\frac{\phi + \psi}{2} \right) \frac{\dot{\theta}}{2} - \sin \frac{\theta}{2} \sin \left(\frac{\phi + \psi}{2} \right) \frac{\dot{\phi} + \dot{\psi}}{2} \tag{A.20}$$

$$\dot{q}_3 = -\sin \frac{\theta}{2} \sin \left(\frac{\phi + \psi}{2} \right) \frac{\dot{\theta}}{2} + \cos \frac{\theta}{2} \cos \left(\frac{\phi + \psi}{2} \right) \frac{\dot{\phi} + \dot{\psi}}{2} \tag{A.21}$$

Thus we obtain the angular velocity using (A.12).

Appendix B

RATTLE algorithm

SHAKE/RATTLE method is used to solve constrained Hamiltonian system.

$$\begin{aligned}
 \mathbf{R}^{n+1} &= \mathbf{R}^n + h\mathbf{P}^{n+1/2}\mathbf{R}^{-1} \\
 \mathbf{P}^{n+1/2} &= \mathbf{P}^n - \frac{h}{2}V_R(\mathbf{R}^n) - h\mathbf{R}^n\boldsymbol{\Lambda}_{(r)} \\
 \mathbf{I} &= [\mathbf{R}^{n+1}]^T\mathbf{R}^{n+1} \\
 \mathbf{P}^{n+1} &= \mathbf{P}^{n+1/2} - \frac{h}{2}V_R(\mathbf{R}^{n+1}) - h\mathbf{R}^{n+1}\boldsymbol{\Lambda}_{(v)} \\
 \mathbf{0} &= [\mathbf{R}^{n+1}]^T\mathbf{P}^{n+1}\mathbf{R}^{-1} + \mathbf{R}^{-1}[\mathbf{P}^{n+1}]^T\mathbf{R}^{n+1}
 \end{aligned}$$

Symplecticity:

$$\begin{aligned}
 d\mathbf{R}^{n+1} &= d\mathbf{R}^n + hd\mathbf{P}^{n+1/2}\mathbf{R}^{-1} \\
 d\mathbf{P}^{n+1/2} &= d\mathbf{P}^n - \frac{h}{2}V_{QQ}(\mathbf{R}^n)d\mathbf{R}^n - hd\mathbf{R}^n\boldsymbol{\Lambda}_{(r)} \\
 d\mathbf{P}^{n+1} &= d\mathbf{P}^{n+1/2} - \frac{h}{2}V_{QQ}(\mathbf{R}^{n+1})d\mathbf{R}^{n+1} - hd\mathbf{R}^{n+1}\boldsymbol{\Lambda}_{(v)}
 \end{aligned}$$

$$\begin{aligned}
 d\mathbf{R}^{n+1} \wedge d\mathbf{P}^{n+1} &= d\mathbf{R}^{n+1} \wedge d\mathbf{P}^{n+1/2} \\
 d\mathbf{R}^{n+1} \wedge d\mathbf{P}^{n+1/2} &= d\mathbf{R}^n \wedge d\mathbf{P}^{n+1/2} \\
 &= d\mathbf{R}^n \wedge d\mathbf{P}^n \\
 \implies d\mathbf{R}^{n+1} \wedge d\mathbf{P}^{n+1} &= d\mathbf{R}^n \wedge d\mathbf{P}^n.
 \end{aligned}$$

Hence this discretisation is Symplectic.

Order of Algorithm: Order of RATTLE algorithm will be defined as minimum of order of discretisation and order of numerical scheme solving non-linear constrained equation B.1. We compare this discretisation with taylor series. From rattle discretisation,

$$\mathbf{R}^{n+1} = \mathbf{R}^n + h \mathbf{P}^n \mathbf{R}^{-1} - \frac{h^2}{2} (V_R(\mathbf{R}^n) + 2\mathbf{R}^n \boldsymbol{\Lambda}_{(r)}) \quad (\text{B.1})$$

From taylor series,

$$\mathbf{R}_{exact}^{n+1} = \mathbf{R}^n + h \left. \frac{d\mathbf{R}}{dt} \right|_{\mathbf{R}^n} + \frac{h^2}{2} \left. \frac{d^2\mathbf{R}}{dt^2} \right|_{\mathbf{R}^n} + O(h^3) \quad (\text{B.2})$$

$$\mathbf{P}_{exact}^{n+1} = \mathbf{P}^n + h \left. \frac{d\mathbf{P}}{dt} \right|_{\mathbf{P}^n} + \frac{h^2}{2} \left. \frac{d^2\mathbf{P}}{dt^2} \right|_{\mathbf{P}^n} + O(h^3) \quad (\text{B.3})$$

$$\left\{ \left. \frac{d\mathbf{R}}{dt} \right|_{(\mathbf{P}^n, \mathbf{R}^n)} \right\}_{ij} = \mathbf{P}_{ik}^n \mathbf{R}_{kj}^{-1} \quad (\text{B.4})$$

$$\begin{aligned} \left\{ \left. \frac{d^2\mathbf{R}}{dt^2} \right|_{(\mathbf{P}^n, \mathbf{R}^n)} \right\}_{ij} &= \frac{d\mathbf{P}_{ik}^n}{dt} \mathbf{R}_{kj}^{-1} \\ &= -(V_R(\mathbf{R}^n) + 2\mathbf{R}^n \boldsymbol{\Lambda}_{(r)})_{ik} \mathbf{R}_{kj}^{-1} \end{aligned} \quad (\text{B.5})$$

Using above two equations and (B.2),

$$\mathbf{R}_{exact}^{n+1} = \mathbf{R}^n + h \mathbf{P}^n \mathbf{R}^{-1} - \frac{h^2}{2} (V_R(\mathbf{R}^n) - 2\mathbf{R}^n \boldsymbol{\Lambda}_{(r)}) + O(h^3). \quad (\text{B.6})$$

Therefore,

$$\|\mathbf{R}_{exact}^{n+1} - \mathbf{R}^{n+1}\| = O(h^3). \quad (\text{B.7})$$

Also,

$$\left. \frac{d\mathbf{P}}{dt} \right|_{(\mathbf{P}^n, \mathbf{R}^n)} = -V_R(\mathbf{R}^n) - 2\mathbf{R}^n \boldsymbol{\Lambda} \quad (\text{B.8})$$

$$\left. \frac{d^2\mathbf{P}}{dt^2} \right|_{(\mathbf{P}^n, \mathbf{R}^n)} = -V_{QQ}(\mathbf{R}^n) \mathbf{P}^n \mathbf{R}^{-1} - 2\mathbf{P}^n \mathbf{R}^{-1} \boldsymbol{\Lambda}_{(v)} \quad (\text{B.9})$$

$$V_R(\mathbf{R}^{n+1}) = V_R(\mathbf{R}^n + h \mathbf{P}^n \mathbf{R}^{-1} + O(h^2)) \quad (\text{B.10})$$

$$= V_R(\mathbf{R}^n) + V_{QQ}(\mathbf{R}^n)(h \mathbf{P}^n \mathbf{R}^{-1}) + O(h^3) \quad (\text{B.11})$$

Hence,

$$\begin{aligned}\mathbf{P}_{exact}^{n+1} &= \mathbf{P}^n - h(V_R(\mathbf{R}^n) + 2\mathbf{R}^n\Lambda_{(v)}) - \frac{h^2}{2}(V_{QQ}(\mathbf{R}^n)\mathbf{P}^n\mathbf{R}^{-1} + 2\mathbf{P}^n\mathbf{R}^{-1}\Lambda_{(v)}) + O(\mathbf{B}^2)2 \\ \mathbf{P}^{n+1} &= \mathbf{P}^n - h(V_R(\mathbf{R}^n) + \mathbf{R}^n\Lambda_{(r)}) - \frac{h^2}{2}(V_{QQ}(\mathbf{R}^n)\mathbf{P}^n\mathbf{R}^{-1}) - h\mathbf{R}^{n+1}\Lambda_{(v)}\end{aligned}$$

From above two equations,

$$\mathbf{P}_{exact}^{n+1} - \mathbf{P}^{n+1} = -2h\mathbf{R}^n\Lambda_{(v)} + h\mathbf{R}^n\Lambda_{(r)} - h^2\mathbf{P}^n\mathbf{R}^{-1}\Lambda_{(v)} + h\mathbf{R}^{n+1}\Lambda_{(v)} \quad (\text{B.13})$$

Hence we conclude that the Rattle algorithm is 2nd order.

Solving Constrained equation: Assuming

$$\bar{\mathbf{R}}^{n+1} = \mathbf{R}^n + h\mathbf{P}^n\mathbf{R}^{-1} - \frac{h^2}{2}V_R(\mathbf{R}^n)\mathbf{R}^{-1} \quad (\text{B.14})$$

and using (B.1),

$$\mathbf{R}^{n+1} = \bar{\mathbf{R}}^{n+1} - h^2\mathbf{R}^n\Lambda_{(r)}\mathbf{R}^{-1}. \quad (\text{B.15})$$

Putting above equation in (B.1)

$$(\bar{\mathbf{R}}^{n+1} - h^2\mathbf{R}^n\Lambda_{(r)}\mathbf{R}^{-1})^T(\bar{\mathbf{R}}^{n+1} - h^2\mathbf{R}^n\Lambda_{(r)}\mathbf{R}^{-1}) - \mathbf{I} = \mathbf{0} \quad (\text{B.16})$$

Let us say

$$f(\Lambda_{(r)}) = (\bar{\mathbf{R}}^{n+1} - h^2\mathbf{R}^n\Lambda_{(r)}\mathbf{R}^{-1})^T(\bar{\mathbf{R}}^{n+1} - h^2\mathbf{R}^n\Lambda_{(r)}\mathbf{R}^{-1}) - \mathbf{I}. \quad (\text{B.17})$$

Then solving (B.16) is equivalent to finding roots of $f(\Lambda_{(r)})$. In case of multiple root and small step size, we take $\Lambda_{(r)}$ with smaller magnitude. Newton-Raphson technique² is used to find roots of $f(\Lambda_{(r)})$.

$$\frac{df(\Lambda_{(r)})}{d\Lambda_{(r)}} = -2h^2A, \quad (\text{B.18})$$

²see Appendix B

where, $[A]_{ij} = [\mathbf{R}^n]_{pi}[\mathbf{R}^{-1}]_{jq}(\bar{\mathbf{R}}^{n+1} - h^2 \mathbf{R}^n \Lambda_{(r)} \mathbf{R}^{-1})_{pq}$. Thus we get the iteration scheme as,

$$\Lambda_{(r)}^{k+1} = \Lambda_{(r)}^k - \left(\frac{df(\Lambda_{(r)})}{d\Lambda_{(r)}} \right)^{-1} \Big|_{\Lambda_{(r)}^k} f(\Lambda_{(r)}^k) \quad (\text{B.19})$$

For initial guess $\Lambda_{(r)}^0$, we solve for the linear terms of (B.1),

$$0 = [\bar{\mathbf{R}}^{n+1}]^T [\bar{\mathbf{R}}^{n+1}] - \mathbf{I} - h^2 \{ [\bar{\mathbf{R}}^{n+1}]^T \mathbf{R}^n \Lambda_{(r)} \mathbf{R}^{-1} + \mathbf{R}^{-T} \Lambda_{(r)}^T \mathbf{R}^{nT} \bar{\mathbf{R}}^{n+1} \} \quad (\text{B.20})$$

$$+ h^4 \mathbf{R}^{-T} \Lambda_{(r)}^T \mathbf{R}^{nT} \mathbf{R}^n \Lambda_{(r)} \mathbf{R}^{-1} \quad (\text{B.21})$$

From (B.16), we see that $[\bar{\mathbf{R}}^{n+1}]^T \mathbf{R}^n = \mathbf{R}^{nT} \bar{\mathbf{R}}^{n+1} = \mathbf{I} + O(h)$. Ignoring h^3 and higher order terms in (B.21) and using symmetry of \mathbf{R}^{-1} and $\Lambda_{(r)}$,

$$0 \approx [\bar{\mathbf{R}}^{n+1}]^T [\bar{\mathbf{R}}^{n+1}] - \mathbf{I} - h^2 \{ \Lambda_{(r)} \mathbf{R}^{-1} + \mathbf{R}^{-1} \Lambda_{(r)} \} \quad (\text{B.22})$$

Thus we get initial guess of $\Lambda_{(r)}$ as

$$\Lambda_{(r),ij}^0 = \frac{1}{h^2} \frac{\mathbf{R}_{ii} \mathbf{R}_{jj}}{\mathbf{R}_{ii} + \mathbf{R}_{jj}} ([\bar{\mathbf{R}}^{n+1}]^T [\bar{\mathbf{R}}^{n+1}] - \mathbf{I})_{ij} \quad (\text{B.23})$$

After getting \mathbf{R}^{n+1} , we solve for $\Lambda_{(v)}$ using (B.1) and (B.1). Let us say

$$\bar{\mathbf{P}}^{n+1} = \mathbf{P}^{n+1/2} - \frac{h}{2} V_R(\mathbf{R}^{n+1}) \quad (\text{B.24})$$

$$\mathbf{0} = [\mathbf{R}^{n+1}]^T \mathbf{P}^{n+1} \mathbf{R}^{-1} + \mathbf{R}^{-1} [\mathbf{P}^{n+1}]^T \mathbf{R}^{n+1} \quad (\text{B.25})$$

$$= [\mathbf{R}^{n+1}]^T \bar{\mathbf{P}}^{n+1} \mathbf{R}^{-1} + \mathbf{R}^{-1} [\bar{\mathbf{P}}^{n+1}]^T \mathbf{R}^{n+1} \quad (\text{B.26})$$

$$-h \{ \Lambda_{(v)} \} \mathbf{R}^{-1} + \mathbf{R}^{-1} \Lambda_{(v)} \} \quad (\text{B.27})$$

Thus, $\Lambda_{(v)} = \{\lambda_{ij}\}$, $\mathbf{R} = \{r_{ij}\}$ and $M = [\mathbf{R}^{n+1}]^T \bar{\mathbf{P}}^{n+1} \mathbf{R}^{-1} + \mathbf{R}^{-1} [\bar{\mathbf{P}}^{n+1}]^T \mathbf{R}^{n+1}$

$$\lambda_{ij} = \frac{r_{ii} r_{jj}}{h(r_{ii} + r_{jj})} M_{ij} \quad (\text{B.28})$$

Appendix C

Proof of Lemma 1

We write angular velocity ω^j as \mathbb{R}^4 vector,

$$\hat{\omega}^j(\mathbf{q}_j, \dot{\mathbf{q}}_j) = [0 \ \omega^T]^T = 2\hat{G}(\mathbf{q}_j)_{4 \times 4}[\dot{\mathbf{q}}_j],$$

where, $\dot{\mathbf{q}}_j = [\dot{q}_{j,0}, \ \dot{q}_{j,1}, \ \dot{q}_{j,2}, \ \dot{q}_{j,3}]^T$ and

$$\hat{G}(\mathbf{q}_j)_{4 \times 4} = \begin{bmatrix} \mathbf{p}^T \\ \mathbf{v}_1^T \\ \mathbf{v}_2^T \\ \mathbf{v}_3^T \end{bmatrix},$$

where, \mathbf{p} , \mathbf{v}_1 , \mathbf{v}_2 and \mathbf{v}_3 are vectors in \mathbb{R}^4 . Vectors \mathbf{v}_2 and \mathbf{v}_3 are defined as

$$\begin{bmatrix} \mathbf{v}_1^T \\ \mathbf{v}_2^T \\ \mathbf{v}_3^T \end{bmatrix} = G(\mathbf{q}_j) = \begin{bmatrix} -q_{j,1} & q_{j,0} & q_{j,3} & -q_{j,2} \\ -q_{j,2} & -q_{j,3} & q_{j,0} & q_{j,1} \\ -q_{j,3} & q_{j,2} & -q_{j,1} & q_{j,0} \end{bmatrix}.$$

Augmented inertia matrix is

$$[\hat{J}]^j = \begin{bmatrix} 1 & 0 & 0 & 0 \\ 0 & J_1^j & 0 & 0 \\ 0 & 0 & J_2^j & 0 \\ 0 & 0 & 0 & J_3^j \end{bmatrix}. \quad (\text{C.1})$$

We want \mathbf{p} to be such that it is perpendicular to $\dot{\mathbf{q}}_j$ (to ensure that first entry of augmented angular velocity $\hat{\omega}^j$ remain 0) and \mathbf{p} is not in span of $\mathbf{v}_1, \mathbf{v}_2$ and \mathbf{v}_3 (to ensure that $\hat{G}(\mathbf{q}_j)^T [\hat{J}]^j \hat{G}(\mathbf{q}_j)$ remain invertible). We have $\mathbf{v}_4 = [q_{j,0} \ q_{j,1} \ q_{j,2} \ q_{j,3}]^T$ perpendicular to $\mathbf{v}_1, \mathbf{v}_2$ and \mathbf{v}_3 . So the general expression for \mathbf{p} not in span of $\mathbf{v}_1, \mathbf{v}_2$ and \mathbf{v}_3 is

$$\mathbf{v} = \alpha_1 \mathbf{v}_1 + \alpha_2 \mathbf{v}_2 + \alpha_3 \mathbf{v}_3 + \alpha_4 \mathbf{v}_4, \quad \alpha_4 \neq 0.$$

\mathbf{p} is perpendicular to $\dot{\mathbf{q}}_j$, i.e.,

$$\mathbf{p}^T \dot{\mathbf{q}} = \alpha_1 \mathbf{v}_1^T \dot{\mathbf{q}} + \alpha_2 \mathbf{v}_2^T \dot{\mathbf{q}} + \alpha_3 \mathbf{v}_3^T \dot{\mathbf{q}} + \alpha_4 \mathbf{v}_4^T \dot{\mathbf{q}} = 0. \quad (\text{C.2})$$

Since $\mathbf{q}_j^T \mathbf{q}_j = 1$, at least one among $q_{j,0}, q_{j,1}, q_{j,2}$ and $q_{j,3}$ is non-zero. Let us assume that $q_{j,3} \neq 0$, then from the constraint $\mathbf{q}_j^T \dot{\mathbf{q}}_j = 0$,

$$\dot{q}_{j,3} = -\frac{1}{q_{j,3}}(q_{j,0}\dot{q}_{j,0} + q_{j,1}\dot{q}_{j,1} + q_{j,2}\dot{q}_{j,2}).$$

Substituting $q_{j,3}$ in C.2,

$$\begin{aligned} & q_{j,0}(\alpha_1(-q_{j,1}q_{j,3} + q_{j,2}q_{j,0}) + \alpha_2(-q_{j,2}q_{j,3} - q_{j,1}q_{j,0}) + \alpha_3(-q_{j,3}^2 - q_{j,0}^2)) \\ & + q_{j,1}(\alpha_1(q_{j,0}q_{j,3} + q_{j,2}q_{j,1}) + \alpha_2(-q_{j,3}^2 - q_{j,1}^2) + \alpha_3(q_{j,2}q_{j,3} - q_{j,0}q_{j,1})) \\ & + q_{j,2}(\alpha_1(q_{j,3}^2 + q_{j,2}^2) + \alpha_2(q_{j,0}q_{j,3} - q_{j,1}q_{j,2}) + \alpha_3(-q_{j,1}q_{j,3} - q_{j,0}q_{j,2})) = 0. \end{aligned}$$

Since this is true for all values of $q_{j,0}, q_{j,1}$ and $q_{j,2}$, their coefficients must be zero. Therefore

$$\begin{bmatrix} q_{j,2}q_{j,0} - q_{j,1}q_{j,3} & q_{j,2}q_{j,3} - q_{j,1}q_{j,0} & -q_{j,3}^2 - q_{j,0}^2 \\ q_{j,0}q_{j,3} + q_{j,2}q_{j,1} & -q_{j,3}^2 - q_{j,1}^2 & q_{j,2}q_{j,3} - q_{j,0}q_{j,1} \\ q_{j,3}^2 + q_{j,2}^2 & q_{j,0}q_{j,3} - q_{j,1}q_{j,2} & -q_{j,1}q_{j,3} - q_{j,0}q_{j,2} \end{bmatrix} \begin{bmatrix} \alpha_1 \\ \alpha_2 \\ \alpha_3 \end{bmatrix} = 0.$$

Only trivial solution is possible for above system of linear equations. We obtain similar result with cases $q_{j,0} \neq 0, q_{j,1} \neq 0$ and $q_{j,2} \neq 0$ respectively. So, the vector $\mathbf{p} = \alpha_4 \mathbf{v}_4$. We take $\alpha_4 = 1$ and write

$$\hat{G}(\mathbf{q}_j) = \begin{bmatrix} q_{j,0} & q_{j,1} & q_{j,2} & q_{j,3} \\ -q_{j,1} & q_{j,0} & q_{j,3} & -q_{j,2} \\ -q_{j,2} & -q_{j,3} & q_{j,0} & q_{j,1} \\ -q_{j,3} & q_{j,2} & -q_{j,1} & q_{j,0} \end{bmatrix}. \quad (\text{C.3})$$

Bibliography

- [1] Softimage. URL http://softimage.wiki.softimage.com/xsidocs/rigidbody_ApplyingRigidBodiesToObjectsasChains.htm.
- [2] Bobby G Sumpter Karl Sohlberg, Robert E Tuzun and Donald W Noid. Application of rigid-body dynamics and semiclassical mechanics to molecular bearings. *IOP Science*, 1997.
- [3] S.P.Norsett E.Hairer and G.Wanner. *Solving Ordinary Differential Equations I - Non-Stiff problems*. Springer Series in Computational Mathematics, 2001.
- [4] Ciro Natale. *Interaction Control of Robot Manipulators: Six-degrees-of-freedom Tasks*. Springer Tracts in Advanced Robotics, 2010.
- [5] Adila. URL <http://www.me.berkeley.edu/~adila/researchNew.htm>.
- [6] Alexander B. Kyatkin Gregory S. Chirikjian. *Engineering Applications of Noncommutative Harmonic Analysis*. CRC Press, 2001.
- [7] Benedict Leimkuhler and Sebastian Reich. *Simulating Hamiltonian Dynamics*. Cambridge University Press.
- [8] P. Steinmann P. Betsch. Constrained integration of rigid body dynamics. *Computer methods in applied mechanics and engineering*, 191:467–488, 2001.
- [9] On quaternions; or on a new system of imaginaries in algebra (letter to john t. graves, dated october 17, 1843). 1843.
- [10] Herbert Goldstein, Charles P. Poole, and John L. Safko. *Classical Mechanics (3rd Edition)*. Addison Wesley, 3 edition, June 2001. ISBN 0201657023. URL <http://www.amazon.com/exec/obidos/redirect?tag=citeulike07-20&path=ASIN/0201657023>.

- [11] Eric P.Fahrendhold Ravishankar Shivarama. Hamiltons equations with euler parameters for rigid body dynamics modeling. *Journal of Dynamic Systems Measurement and Control*, 126:Page 124, 2004.
- [12] Peter Betsch and Ralf Siebert. Rigid body dynamics in terms of quaternions: Hamiltonian formulation and conserving numerical integration. *International Journal for Numerical Methods in Engineering*, 79(4):444–473, 2009. ISSN 1097-0207. doi: 10.1002/nme.2586. URL <http://dx.doi.org/10.1002/nme.2586>.
- [13] Aaron D. Schutte Firdaus E. Udwadia. A unified approach to rigid body rotational dynamics and control. *Proceedings of the Royal Society A*, doi:10.1098/rspa.2011.0233, 2001.
- [14] Loup Verlet. Computer "experiments" on classical fluids. i. thermodynamical properties of lennard-jones molecules. *Phys. Rev.*, 159:98–103, Jul 1967. doi: 10.1103/PhysRev.159.98. URL <http://link.aps.org/doi/10.1103/PhysRev.159.98>.
- [15] S.P.Norsett E.Hairer and G.Wanner. *Geometric numerical integration*. Springer Series in Computational Mathematics, 2001.
- [16] Basant Lal Sharma. Lecture notes in hamiltonian mechanics and symplectic algorithms. 2011.
- [17] Peter Betsch Ralf Siebert. Numerical integration of rigid body dynamics in terms of quaternions. *Proceedings in Applied Mathematics and Mechanics*, Volume 8, Issue 1: 1013910140, December 2008.
- [18] P. Betsch Stefan Uhlar. Energy consistent time integration of non-conservative hybrid multibody systems. In *Proceedings of the ASME 2009 International Design Engineering Technical Conferences & Computers and Information in Engineering Conference*, 2009.
- [19] Jerrold E. Marsden1 Sigrid Leyendecker and Michael Ortiz. Variational integrators for constrained dynamical systems. *Zeitschrift fr Angewandte Mathematik und Mechanik*, 88:677–708, 2008.
- [20] P. Betsch Stefan Uhlar. On the derivation of energy consistent time stepping schemes for friction afflicted multibody systems. *Computers and Structures*, 88:737–754, 1 April, 2010.

- [21] V.I. Arnold. *Mathematical Methods of Classical Mechanics*. Graduate Texts in Mathematics, 1989.
- [22] Loring W.Tu. *An Introcution to Manifolds*. Sprin, 2011.
- [23] Peter A. Kollman Shuichi Miyamoto. Settle: An analytical version of the shake and rattle algorithm for rigid water models. *Journal of Computational Chemistry*, 13:952–962, October 1992.
- [24] J.E. Jones. On the determination of molecular fields. i. from the variation of the viscosity of a gas with temperature. *Proceedings of the Royal Society A*, 106:441–462, 1924.